

PERFORMANCE OF NEAR INFRARED DIGITAL IMAGING  
TRANSILLUMINATION FOR DETECTION OF  
NON-CAVITATED APPROXIMAL CARIES

by

Naif Nabel Fouad Abogazalah

Submitted to the Graduate Faculty of the School of  
Dentistry in partial fulfillment of the requirements  
for the degree of Master of Science in Dentistry,  
Indiana University School of Dentistry, June 2016.

Thesis accepted by the faculty of the Departments of Cariology, Operative Dentistry, and Dental Public Health, Indiana University School of Dentistry, in partial fulfillment of the requirements for the degree of Master of Science in Dentistry.

---

Kim Diefenderfer

---

Jeffrey A. Platt

---

Masatoshi Ando  
Chair of the Committee

---

Anderson T. Hara  
Program Director

---

N. Blaine Cook  
Program Director

---

Date

DEDICATION

This thesis is dedicated to those who without their prayers, love and support, my professional growth would not have been possible: my mother, Halimah, and my father, Nabel.

I would also like to dedicate this work to my brothers Bader, Fouad, Mohammad, Faisal, and Khalid, and my dearest sister, Noof, for their continuous support and encouragement.

## ACKNOWLEDGMENTS

I first have to thank King Khalid University for giving me this opportunity to further my career in Operative Dentistry and for the Saudi Ministry of Education for their financial grant and their support throughout my course of studies.

Next, I would like to convey my deepest appreciation and thanks to my research committee, Drs. Masatoshi Ando, Anderson T. Hara, Norman B. Cook, Jeffrey A. Platt, and Kim E. Diefenderfer for their professionalism and support.

Special thanks go to Dr. N. Blaine Cook who taught, challenged, and encouraged me through the Operative Dentistry studies.

I thank Dr. Masatoshi Ando, for his guidance and thoughtful criticism, which allowed me to appreciate scientific integrity. His guidance helped me during all research and writing phases of this thesis as a research mentor.

I would like to extend thanks to fellow classmates Drs. Nasreen El-ezmerli, Fahad Binsaleh and Matthew Rouse, for their friendship and support during this program.

I would like to thank the people without whom this project would not be accomplished. Special thanks to Dr. James C Williams, Department of Anatomy and Cell Biology, Indiana University School of Medicine, for making me feel welcome, and for allowing me to use their Skyscan microfocus computed tomography machine. I extend my deep thanks to Dr. Edwin T. Parks, Department of Oral Pathology, Medicine, and Radiology, Indiana University School of Dentistry, for providing the x-ray beam-aiming device, and for the enriching discussion regarding dental radiography. I thank Drs. Kenneth J. Spolnik and Josef Bringas, Department of Endodontics, Indiana University

School of Dentistry, for allowing me to use their digital radiography system. I would like to thank Mr. George Eckert, who assisted with the statistical analysis of the data. Finally, in addition to Drs. Hara and Ando, I extend my deep appreciation to Dr. Ana Gossweiler for her time, help, and suggestions in support of this project.

This study was partially supported by a grant from Delta Dental Foundation (Okemos, MI) and the Oral Health Research Institute, Indiana University School of Dentistry, Indianapolis, Indiana.

TABLE OF CONTENTS



INTRODUCTION .....	1
REVIEW OF LITERATURE .....	8
METHODS AND MATERIALS .....	19
RESULTS .....	29
FIGURES AND TABLES .....	32
DISCUSSION .....	55
SUMMARY AND CONCLUSION .....	62
REFERENCES .....	65
APPENDIX .....	83
ABSTRACT .....	99
CORRICULUM VITAE	

LIST OF ILLUSTRATIONS

FIGURE 1	Near Infrared Digital Imaging Transillumination device system components . . . . .	33
FIGURE 2	Illustration of Near Infrared Digital Imaging Transillumination . . . . .	34
FIGURE 3	Near Infrared Digital Imaging Transillumination image of a premolar with approximal caries lesion . . . . .	35
FIGURE 4	Flow chart of the study. . . . .	36
FIGURE 5	Skyscan 1172 high resolution microfocus computed tomography machine . . . . .	37
FIGURE 6	Sample distribution flow chart . . . . .	38
FIGURE 7	Sample assembly on Lego <sup>®</sup> bricks . . . . .	39
FIGURE 8	Custom film holder with beam aiming device. . . . .	40
FIGURE 9	Digital Imaging Fiber Optic Transillumination (DIFOTI) images Acquisition . . . . .	41
FIGURE 10	Graph demonstrating intra-examiner repeatability and inter-examiner agreements of the methods . . . . .	42
FIGURE 11	Graph demonstrating overall sensitivity and specificity of the methods . . . . .	43
FIGURE 12	Graph demonstrating overall sensitivity of the methods at different thresholds . . . . .	44
FIGURE 13	Graph demonstrating receiver operating characteristic curves of all methods . . . . .	45
FIGURE 14	Graph demonstrating Spearman correlation coefficient of the methods . . . . .	46
TABLE I	Microfocus computed tomography scoring criteria . . . . .	47

TABLE II	International Caries Detection and Assessment System, ICDAS-II scoring criteria . . . . .	48
TABLE III	Radiography scoring criteria . . . . .	49
TABLE IV	Digital Imaging Fiber Optic Transillumination scoring criteria . . . . .	50
TABLE V	Near Infrared Digital Imaging Transillumination scoring criteria . . . . .	51
TABLE VI	Intra-examiner repeatability and inter-examiner agreements . . . . .	52
TABLE VII	Specificity, sensitivity, area under receiver operating characteristic curve . . . . .	53
TABLE VIII	Spearman correlation coefficient of the methods . . . . .	54

## INTRODUCTION

It has been known that demineralization and remineralization of tooth structure occur over time. More importantly, the net balance between the pathologic and protective factors will determine the rate of caries lesion progression to a state that can be detected visually or by other caries detection methodologies.<sup>1-5</sup>

As a result of the widespread use and availability of fluoride, caries lesion behavior has changed significantly and a lower progression rate has been observed.<sup>6,7</sup> The slow progress of the caries lesion gives the dental professional a substantial opportunity to diagnose and manage dental caries at an early stage, as non-cavitated lesions can be arrested or remineralized before irreversible destruction of the tooth structure occurs.<sup>1,5,8</sup> Hence, early caries detection and monitoring can have a profound effect on the success of preventive treatment of non-cavitated caries lesions.<sup>5</sup>

Occlusal, approximal, and free smooth surfaces at the gingival margins of the teeth are susceptible to dental caries, as caries lesions develop in areas of stagnation where plaque can accumulate undisturbed.<sup>9</sup> Epidemiological studies in children, young adults and adults have shown a shift in caries prevalence from occlusal surfaces at younger age to approximal surfaces at adulthood.<sup>10-15</sup> Unlike the occlusal and free smooth surfaces, the approximal surfaces cannot be visualized directly due to presence of neighboring teeth. Therefore, clinicians commonly rely on bitewing radiographic signs of demineralization for early approximal caries detection and for caries lesion monitoring over time.<sup>16-18</sup>

Visual caries examination is the most frequently used method for caries detection in daily dental practice.<sup>19, 20</sup> This is perhaps because it is an expedient technique with no additional cost to the dentist and the patient.<sup>20, 21</sup> The main limitation of visual caries detection is related to its subjective nature,<sup>20, 21</sup> thus interpretation of clinical signs of caries lesions may vary among examiners.<sup>19, 20</sup> Studies evaluating visual examination for caries detection have reported results with an extensive range of sensitivity (Sn) and specificity (Sp) values.<sup>19, 20</sup> This wide variation in the results among studies may be at least partially due to the vast array of classification criteria, as well as differences in the conditions under which the examinations were performed.<sup>20, 22</sup> Consequently, an effort has been made to develop and validate visual caries detection systems<sup>23-25</sup> such as the International Caries Detection and Assessment System (ICDAS).<sup>26</sup> ICDAS records dental caries using an ordinal scale from 0 to 6 in an attempt to correlate the clinical appearance of the teeth to their histological status.<sup>26-28</sup> ICDAS has been shown in vitro to be more reliable and accurate than radiographic examination for detecting and estimating the depth of early approximal lesions when the approximal surface was visualized directly.<sup>29</sup>

Gimenez et al.,<sup>30</sup> performed a systematic review with meta-analysis to discern the overall performance of visual examination for caries detection. They found that studies that used firmly established scoring criteria demonstrated higher accuracy in approximal and occlusal caries detection than studies that did not report the scoring method or that used non-validated scoring systems.<sup>30</sup> Additionally, since Sn and Sp are the most commonly used indicators of diagnostic test performance, they calculated Sn and Sp from published literature at two thresholds: “initial caries lesion” which defined as “all lesions independent of lesion depth or dental surface integrity,” and “more advanced caries

lesions” which defined as lesion extended to dentin or cavitated lesions. Regarding “initial caries lesion” detection, they found that the Sn *in vivo* was 0.297 and Sp was 0.990 in permanent teeth, and 0.430 and 0.908, respectively, in primary teeth. *In vitro* the Sn was 0.715 and Sp was 0.796 in permanent teeth, while in primary teeth Sn was 0.709 and Sp was 0.865. They mentioned that the discrepancies between *in-vivo* and *in-vitro* studies may be related to the presence of saliva and dental soft tissues, which may reduce caries detection ability, leading to lower Sn values *in vivo*.<sup>30</sup> Also, difficulty in reassembling the approximal contact *in vitro* could be a possible explanation.<sup>31</sup> Nevertheless, visual examination possesses limited accuracy for early approximal caries detection.<sup>32</sup> Therefore, additional methods, such as radiography, are likely to be used.<sup>33</sup>

First described by Raper (1925), bitewing radiography in combination with visual examination has become the traditional method for approximal caries detection.<sup>16, 17, 34</sup> Radiographs also help to estimate approximal and occlusal caries lesion depth and enable detection of lesions on visually inaccessible surfaces.<sup>16, 34</sup> Based on a recent systematic review with meta-analysis,<sup>35</sup> radiographic examination has shown in *in-vivo* studies to be suitable for detecting cavitated approximal caries lesions; Sn ranged from 0.59 to 0.70 and Sp ranged from 0.97 to 0.99. However, with low Sn (ranging from 0.21 to 0.26) for detecting early approximal enamel and dentin lesions, diagnostic inaccuracy of bitewing radiography remains a problem (for review, please see<sup>35</sup>)

A further limitation of radiographic caries detection is that image interpretation may vary significantly within or between examiners.<sup>16, 36, 37</sup> Also, some technical factors may adversely affect the quality of bitewing radiography. Errors in vertical and horizontal angulation of the x-ray tube head, film, and film holder can lead to under- or



over-estimation of the lesion depth.<sup>16, 34, 38-40</sup> Moreover, difficulty in reproducing projection geometry limits the ability to assess lesion progression over time.<sup>16</sup> In addition to errors related to technical factors, several operator variables may also affect the diagnostic ability of dental radiography. Image noise, such as structure noise<sup>41-43</sup> and quantum noise<sup>41</sup> lowers the precision of radiographic images. Geometry of the caries lesion,<sup>44</sup> radiopacity of adjacent restorative materials,<sup>44-48</sup> cervical burnout and Mach band effect,<sup>49</sup> and viewing condition<sup>50</sup> can also limit diagnostic accuracy.

An argument has been raised to re-evaluate clinicians' over-reliance on using radiography for caries detection because of the following reasons: (1) decrease in caries prevalence,<sup>16</sup> (2) slow progression rate of approximal caries lesions as the result of the widespread use of fluoride,<sup>6, 7</sup> (3) the risk associated with low-dose radiation, especially for children.<sup>16</sup> Although there is no conclusive evidence that dental radiographs taken during childhood increase the risk of malignant diseases,<sup>51, 52</sup> it is still difficult to justify the repeated use of bitewing radiography to monitor caries lesions; or to evaluate the effectiveness of non-invasive dental preventive treatments.<sup>16, 19, 53-55</sup> Therefore, because of these concerns, it is of vital importance to continue the development of new caries detection techniques with improved, Sn, Sp, and reliability, and with no additional risk to the patients.

Searching for a better caries detection method has resulted in many attempts. Methods based on light transillumination have been improved. Digital imaging fiber optic transillumination (DIFOTI) (Electro-Optical Sciences Inc., NY, USA) was introduced as a more sensitive, non-irradiative adjunctive method for early caries detection.<sup>56</sup> However,

due to its high price, DIFOTI, has not been widely used,<sup>57</sup> and a new less expensive generation of transillumination techniques has been introduced.<sup>58</sup>

Using the same principle of transillumination as in DIFOTI, Near Infrared Digital Imaging Transillumination (NIDIT) was introduced in Europe as DIAGNOcam (KaVo, Biberach, Germany) in 2012, and a year later, in the United States as CariVu™ (DEXIS, LLC, Hatfield, PA, USA).<sup>58</sup> Instead of using visible light like DIFOTI, this device uses a near infrared (wave length ~ 780 nm) light to transilluminate the tooth. The system (Figure 1) consists of a charged coupled device (CCD) sensor to capture images, connection to a computer, special software, and elastic arms containing a near infrared light source that transmits light through the gingiva, the alveolar bone, the root of the tooth, and up to the crown (Figure 2). The image is displayed from the occlusal and saved in digital format (Figure 3).<sup>58</sup>

Kuhnisch J et al.,<sup>59</sup> performed an *in-vivo* study to compare the performance of visual examination, radiography, Laser Fluorescence pen (LF pen, DIAGNOdent Pen, KaVo Biberach, Germany) and NIDIT for detection of dentin-involved approximal caries lesions. The Sn values were 0.016 for visual, 0.667 for LF pen, 0.992 for NIDIT, and 0.961 for radiography.<sup>59</sup> This study demonstrated the potential of NIDIT for approximal caries detection.

To our best knowledge, no study has evaluated NIDIT imaging for measuring the extension of lesion depth, validity and reliability. Hence, we observed the need for *in-vitro* validation of NIDIT regarding the detection of early non-cavitated caries lesions. This *in-vitro* model should be established to simulate the clinical situation in terms of

allowing the near infrared light to be transmitted through a certain material thickness and the roots up to the crown of the tooth.

### Objectives

The objectives of this study were:

1. To evaluate the ability of the NIDIT to detect non-cavitated enamel and dentin approximal caries lesions.
2. To compare the performance among the NIDIT, ICDAS, digital radiography (DR), and DIFOTI.

### Null Hypotheses

The null hypotheses of this study were 1) NIDIT cannot detect non-cavitated enamel and dentin approximal caries lesions, and 2) No difference exists in the performance among the NIDIT, ICDAS, DR, and DIFOTI.

### Alternative Hypotheses

The alternative hypotheses of this study were 1) The NIDIT imaging system can detect non-cavitated enamel and dentin approximal caries lesions, and 2) A difference exists in the performance among NIDIT, ICDAS, DR, and DIFOTI.

REVIEW OF LITERATURE

In addition to visual/tactile examination and bitewing radiography, several adjunctive methods have been used for approximal caries detection. Examples include tooth separation, fiber optic transillumination (FOTI), digital imaging fiber optic transillumination (DIFOTI, Electro-Optical Sciences Inc, NY, USA), cone beam computed tomography (CBCT), optical coherence tomography (OCT), laser fluorescence (DIAGNOdent, KaVo, Biberach, Germany), ultrasound, light emitting diode (LED) fluorescence (Midwest Caries I.D.<sup>TM</sup>), frequency-domain photothermal radiometry and modulated luminescence (PTR/LUM, The Canary System ®, Quantum Dental Technologies Inc., Toronto, Ontario, Canada).

#### TOOTH SEPARATION

Temporary tooth separation was advocated as it offers dentists a chance to determine whether the lesion is cavitated, active or inactive, especially in children and low caries risk and motivated patients.<sup>17,20</sup> Tooth separation was introduced more than a century ago.<sup>60</sup> It has been taught in a number of dental schools across Europe.<sup>61</sup>

Temporary tooth separation requires two appointments. At the first, an orthodontic elastic band is placed between the approximal surfaces to be diagnosed. The second appointment is 3 to 7 days later. At this appointment, the separator is removed, revealing a widened interproximal space that can be examined.<sup>16,62</sup> Space closure occurs spontaneously within 48 hours of separator removal.<sup>63</sup> Several studies have demonstrated that more approximal caries lesions were detected at much earlier stages when tooth

separation was performed.<sup>7, 64, 65</sup> Temporary tooth separation can confirm presence or absence of cavitation and increases access for conservative restorations and preventive agent placement.<sup>7, 66-73</sup> However, tooth separation may not always result in improved accessibility for direct examination of the approximal lesion, and may cause discomfort to the patient. Also, it requires an extra visit for the patient.<sup>16, 65</sup> Thus, the use of tooth separation has not yet gained popularity as a routine method for approximal caries detection in the dental office.<sup>16, 60, 74</sup>

#### FIBER OPTIC TRANS ILLUMINATION (FOTI) AND DIGITAL IMAGING FIBER OPTIC TRANSILLUMINATION (DIFOTI)

FOTI is a simple technique that uses a narrow beam white light to transilluminate the tooth. Friedman and Marcus<sup>75</sup> suggested this technique for caries detection. The principle behind FOTI is when areas of disrupted enamel crystals that occur in demineralized tooth tissues are transilluminated, they appear as dark shadows due to changes in the light scattering and absorption of light photons.<sup>75</sup>

The Sn of FOTI has been shown to vary between 0.50 and 0.85<sup>76, 77</sup> with higher Sn value for dentin lesions than for enamel lesions.<sup>78-80</sup> Peers et al.,<sup>81</sup> compared *in vitro* the performance of radiography and FOTI using histologic examination as a gold standard. They found no significant difference between the Sn values of radiography (0.59) and FOTI (0.67) regarding the approximal caries detection. Although, FOTI is widely accepted by clinicians to detect approximal caries in anterior teeth, it also may add substantially to dentin-involved caries detection in posterior teeth.<sup>20</sup>

DIFOTI uses the same principle as FOTI. DIFOTI uses a visible light (wavelength range between 450 and 700 nm) to transilluminate the tooth and a charge

coupled device (CCD) camera. DIFOTI can capture a real time image from occlusal (DIFOTI-Occlusal) or buccal and lingual surfaces (DIFOTI-BL).

Schneiderman et al.,<sup>56</sup> compared DIFOTI with radiography in an *in-vitro* study with histologic examination as a gold standard. DIFOTI showed a higher Sn (0.56), but lower Sp (0.76), than radiography, which showed Sn and Sp values of 0.21 and 0.91, respectively. Moreover, DIFOTI was shown *in vivo* to have higher Sn than visual examination for detection of cavitated approximal lesions when visual examination after cavity preparation was used as a reference standard.<sup>82</sup> Furthermore, DIFOTI has shown a correlation between the degree of darkened shadow and the lesion depth in occlusal and smooth surface lesions *in vivo*.<sup>83</sup> Hence, it demonstrates a potential to provide objective data for caries lesion assessment as gray scale value may be used for this purpose.<sup>83</sup>

DIFOTI offers several advantages over bitewing radiography, including: (1) elimination of the radiation hazard associated with bitewing radiography; (2) images are viewed in real time; (3) no film, which reduces patients' discomfort associated with the use of intra-oral films or sensor; and (4) higher Sn than radiography for early caries detection.<sup>56, 81, 84</sup> The disadvantages of DIFOTI are as follows: (1) it has not been proven that DIFOTI can objectively quantify lesion size, depth, volume, and mineral content; (2) DIFOTI cannot differentiate between caries lesions and developmental defects such as fluorosis; (3) DIFOTI does not determine caries activity; and (4) the higher Sn value might lead to higher false positive values, which might lead to over-treatment.

#### CONE BEAM COMPUTED TOMOGRAPHY (CBCT)

CBCT is a modification of medical computed tomography (medical CT), which uses cone beam of x-rays rather than fan beam in the conventional medical CT. CBCT

generates three-dimensional (3D) images at lower radiation doses and lower cost than the conventional medical CT. The subsequent 3D image can be sectioned using imaging software and viewed in frontal, sagittal, and axial planes. CBCT has been used for several dental diagnostic purposes, such as dental implant treatment, craniofacial anomalies, endodontics, orthodontics, and periodontics.<sup>85-90</sup> Several studies have reported the use of CBCT for enamel and dentin caries detection.<sup>91-104</sup> The majority of these studies were *in vitro* and compared the performance of CBCT with conventional or digital intraoral radiography and histology or micro computed tomography (micro-CT) as a gold standard. Most of these studies have shown that CBCT does not improve the accuracy of caries detection when compared with conventional or digital intraoral radiography.<sup>91-93, 95, 96, 105</sup>

Regarding cavitated approximal caries detection, CBCT demonstrated a significantly higher Sn than intraoral conventional and digital radiography *in vivo*.<sup>106</sup> In this *in-vivo* study, direct visual inspection of the approximal surface after tooth separation was used as a reference standard. However, none of the included teeth had metallic restorations; thus, they are less likely to show beam hardening artifact, which has a profound effect on the quality of CBCT images. In addition to beam hardening artifacts, the higher cost and higher radiation dose of the CBCT compared to intraoral radiography limit its use as a primary radiographic modality for dental caries detection.<sup>107</sup>

#### OPTICAL COHERENCE TOMOGRAPHY (OCT)

Optical coherence tomography (OCT) is a novel non-invasive, non-irradiative imaging technique that uses infrared light to produce a real time cross-sectional image of a tissue. OCT constructs images from the back-scattered light of a transilluminated tissue based on the differences of the optical absorption and scattering properties of the tissue.



<sup>108, 109</sup> OCT has been used in several clinical applications, including dermatology,<sup>110, 111</sup> gastroenterology,<sup>112</sup> ophthalmology<sup>113</sup> and dentistry<sup>109, 114, 115</sup> OCT in dentistry can be used for early caries detection,<sup>114</sup> tooth crack diagnosis,<sup>116</sup> and assessment of marginal integrity of existing restorations.<sup>117, 118</sup>

Swept-source optical coherence tomography (SS-OCT) is an improved modification of traditional OCT systems. One *in-vivo* study evaluated the performance of SS-OCT and bitewing radiography for approximal caries detection.<sup>114</sup> The reference standard was based on information collected from direct visual examination before caries excavation, visual examination after caries excavation, radiography, and SS-OCT. SS-OCT demonstrated significantly higher Sn and Sp than radiography for enamel and outer one-third dentin caries detection.<sup>114</sup> However, for deep dentin caries, SS-OCT produced significantly lower Sn than radiography, while the Sp was the same. This is due to significantly greater SS-OCT beam attenuation and scattering in dentin than in enamel.<sup>115</sup> Also, in this study, pulp chambers did not appear clearly in the OCT images; therefore, lesion depth in relation to the pulp could not be determined. This is an important clinical shortcoming, especially in the case of symptomatic teeth.

#### LASER FLUORESCENCE (DIAGNODENT)

Laser Fluorescence (LF) caries detection (DIAGNOdent, KaVo Biberach, Germany) is based on the principle that when a red light (wavelength ~ 655 nm) is applied to a tooth, the caries-related changes in the tooth tissues lead to an increase in fluorescence.<sup>119</sup> It was suggested that these changes in fluorescence are due to protoporphyrin, a photosensitive pigment present in carious tissues as a result of bacterial metabolic activities.<sup>120</sup> Clean and healthy teeth produce little or no fluorescence, while

carious teeth produce fluorescence proportional to the degree of caries.<sup>121</sup> LF provides values from a point of application that can be used to estimate the depth of the caries lesion. These values range from 0 to 99. For example, scores from 0-10 might be interpreted as healthy and scores above 30 might indicate a lesion that requires restorative treatment.<sup>57, 122</sup> A laser fluorescence pen (LF pen) (DIAGNOdent Pen, KaVo Biberach, Germany) was introduced with a smaller tip design to allow detection of approximal caries lesions. Lussi and Hellwig<sup>130</sup> reported performance similar to the traditional DIAGNOdent on occlusal surfaces. Ribeiro et al.<sup>123</sup> evaluated the performance of visual examination, bitewing radiography, and LF pen for detection of approximal caries on primary teeth *in vivo*; micro-CT served as a gold standard after the teeth were exfoliated.<sup>123</sup> Before tooth separation, the LF pen demonstrated higher Sn, but lower Sp, than visual and bitewing radiographic examinations for detection of enamel caries. For dentin lesions, the Sn of LF pen was higher than visual examination but lower than bitewing radiography, and the Sp was significantly lower than both visual examination and bitewing radiography. Tooth separation significantly improved the Sn and Sp values of visual and LF pen examinations for detection of both enamel and dentin caries lesions. For enamel caries, visual examination provided higher Sn, while LF pen showed significantly higher Sn for dentin caries detection. After tooth exfoliation, they performed *in-vitro* LF pen examination and it showed improved Sn and Sp for both enamel and dentin lesions because the laser light could directly access the tooth surface.<sup>123</sup> A systematic review of DIAGNOdent<sup>124</sup> concluded that LF has higher Sn than other traditional diagnostic methods. However, LF has a higher tendency to produce false-positive diagnoses, which suggests that it should be used with caution and not as a

primary diagnostic method.<sup>121</sup>

## ULTRASOUND

The use of diagnostic ultrasound in dentistry was first reported more than 50 years ago.<sup>125</sup> Ultrasound uses sound waves with higher frequency than humans are able to hear.<sup>126</sup> This frequency limit is approximately 20 kilohertz. Ultrasound imaging offers several advantages, as it is simple, low-cost, with no harmful side effects, and it can provide a real time images.<sup>127</sup> For caries detection, ultrasound is based on the substantial difference in sonic conductivity between sound and demineralized enamel.<sup>127</sup> An *in-vitro* study evaluated an ultrasonic caries detection device and radiography for cavitated approximal caries detection with histology as a gold standard.<sup>128</sup> Both the Sn and Sp of the ultrasonic caries detection device were 1.00, while for radiography the Sn was 0.90 and Sp 0.92.<sup>128</sup> *In vivo*, the same ultrasonic device system produced a mean Sn (by three examiners) of 0.82 and Sp of 0.75 for cavitated approximal caries detection (visual examination after cavity preparation was used as the reference standard.)<sup>129</sup> For radiography, the mean Sn and Sp were 0.49 and 0.90. The authors suggested that the specificity of the device can be improved by enhancing the ultrasound signal processing algorithm to reduce false positive diagnoses.<sup>129</sup> Although, the ultrasonic caries detection device showed promising results, there are no further studies reporting the use of this system.

## LIGHT EMITTING DIODE (LED) FLUORESCENCE (MIDWEST CARIES I.D.<sup>TM</sup>)

The principle of this method is that it detects differences in the reflection and refraction of infrared energy from red light-emitting diodes (LED) that is carried by a fiber optic cable to a tooth. The presence of a caries lesion will lead to changes in these

properties. Another fiber optic cable serves as a photodetector that transmits captured light to a microprocessor, which compares the signals to defined parameters.<sup>130</sup> A Caries detection method based on this principle was introduced as Midwest Caries I.D.<sup>TM</sup> (Dentsply, York, PA, USA).

One *in-vitro* study<sup>131</sup> evaluated the performance of LED Fluorescence, LF pen, radiography, and visual examination for approximal enamel and dentin caries detection. Visual examination and radiography performed better in terms of Sn and Sp for both enamel and dentin lesions. The authors concluded that LED fluorescence was not adequate for approximal caries detection, perhaps due to loss of signal during signal transduction through the occlusal part of the lesion.<sup>131</sup>

#### FREQUENCY-DOMAIN INFRARED PHOTOTHERMAL RADIOMETRY AND MODULATED LUMINESCENCE (PTR/LUM, THE CANARY SYSTEM<sup>®</sup>)

The Canary System<sup>®</sup> (Quantum Dental Technologies Toronto, Ontario, Canada) is based on photothermal radiometry and modulated luminescence technology (PTR/LUM). The manufacturer claims that this system: (1) can detect caries from 50  $\mu\text{m}$  to 5 mm depth, including caries under sealants and around the margins of restorations; (2) is not affected by stains or calculus, and (3) does not require a dry field.

PTR is based upon the modulated thermal infrared response (black body or Plank radiation) of a medium that results from repeated irradiation of a specimen.<sup>132-134</sup> Black body radiation is a type of electromagnetic radiation surrounding or within a body in thermodynamic equilibrium with its environment or emitted by a black body when the temperature is uniform and constant. The radiation has a specific constant and intensity dependent only on the temperature of the body.<sup>132-134</sup> A change in the temperature of the

sample surface will occur as a result of the conversion of the absorbed radiation energy to thermal energy. The change in the thermal emissions caused by the modulated temperature can be measured using an infrared detector that constitutes the PTR signal.<sup>132, 134</sup>

LUM is based on the conversion of optical energy to radiation energy. When a molecule absorbs optical energy from a laser source, it results in excitation of its chromophores to a higher energy state, then de-excitation to a lower energy state, and longer wavelength energy is emitted. This emitted longer wavelength can be detected via a photodetector, which constitutes the LUM signal.<sup>132, 134</sup>

The PTR/LUM caries detection method has demonstrated higher Sn and Sp than visual examination, radiography, and DIAGNOdent for early occlusal caries detection.<sup>135</sup> For early approximal caries detection, PTR has shown an increase in the amplitude by more than 300% after 80 hours of artificial demineralization. However, LUM was found to have lower ability than PTR to detect early approximal lesions.<sup>136</sup> An *in-vitro* study evaluated the performance of PTR/LUM, visual examination, and radiography, with polarized light microscopy as a gold standard for approximal caries detection. The Sn of PTR/LUM was higher than both visual examination and radiography. There was no significant difference in Sp between PTR/LUM and radiography, but visual examination was significantly lower.<sup>137</sup> The PTR/LUM method is still new and further studies are needed to evaluate its performance.

#### MICROFOCUS COMPUTED TOMOGRAPHY (M-CT)

In order to calculate Sn and Sp of a diagnostic test, a gold standard must be established.<sup>138</sup> Traditionally, histological examination of sliced tooth sections has been

used for this purpose.<sup>138</sup> However, histological examination has several limitations. Mechanical sectioning of the teeth may damage the caries site. Also, the sectioned slice may not resemble the real extension of the lesion or the corresponding examined site, which may result in under- or over-estimation of the lesion extension. Further, this method requires destruction of specimens, which excludes the possibility for *in-vitro* monitoring of the lesion.<sup>139-141</sup>

On the other hand, microfocus computed tomography ( $\mu$ -CT) allows non-destructive 3D visualization of the morphological characteristics of teeth and the determination of the mineral content in teeth and bones.<sup>142-149</sup>  $\mu$ -CT is a microscopic version of the medical CT. A major difference between  $\mu$ -CT systems and medical CT scanners is that, in the  $\mu$ -CT units, the specimen moves while the x-ray source and detector are stationary.<sup>142</sup> The basic components of  $\mu$ -CT are: (1) an X-ray source, and (2) a detector that receives attenuated X-rays from an irradiated object.<sup>150, 151</sup> The principle of  $\mu$ -CT is based upon mathematical reconstruction of the linear attenuation coefficient from measurements of attenuated X-ray beams that pass through an object at different angles.<sup>150, 151</sup> The linear attenuation coefficient depends on photon energy, chemical composition, and density of the material.<sup>150, 151</sup>

$\mu$ -CT has been used as a gold standard for validation of diagnostic performance of different caries detection methods in several studies.<sup>98, 123, 152, 153</sup> In addition to the nondestructive characteristic of  $\mu$ -CT, the main advantage of  $\mu$ -CT validation is the ability to examine countless numbers of tooth sections; therefore, it allows determining the actual lesion site and depth.<sup>153</sup>

## METHODS AND MATERIALS

## TEETH SELECTION

Figure 4 illustrates a flow of the current study. Eighty-five teeth were selected from a pool of extracted teeth. They included twelve sound, as well as 73 carious premolars that had approximal non-cavitated caries lesions surrounded by sound enamel. The presence of caries was determined by visual tooth surface changes.<sup>20</sup> The extracted human teeth were collected from dental practitioners across the United States. The collection of human teeth for use in dental laboratory research studies has been approved by the Indiana University (IU) Institutional Review Board (IU-IRB#:1512034387). All specimens were stored in 0.1% thymol solution at 4° C until used. Teeth were cleaned using a Robinson's brush with water on a slow speed handpiece.

## INITIAL MICROFOCUS COMPUTED TOMOGRAPHY (M-CT) IMAGE ACQUISITION

The selected eighty-five teeth were mounted and secured on plastic Lego<sup>®</sup> bricks (The LEGO Group, Billund, Denmark) using utility wax (Heraeus Kulzer Inc., Lafayette, IN, USA). The teeth were scanned using microfocus computed tomography ( $\mu$ -CT) to establish a gold standard assessment. The  $\mu$ -CT images were acquired using Skyscan  $\mu$ -CT machine (Figure 5) (Skyscan 1172, Kontich, Belgium) at 80 kV, 134  $\mu$ A, 8.9  $\mu$ m pixel size resolution. An Al + Cu filter was used. The specimens were rotated at 180° with rotation step of 0.7° and frame average of 4. Three-dimensional (3D) image reconstruction was done using NRecon version 1.6.6 software (Bruker microCT, Kontich, Belgium). The reconstructed images were stored in 16-bit TIFF files. Visual



interpretation of sagittal views of the  $\mu$ -CT images was performed using image display software (CT-Analyzer, Bruker microCT, Kontich, Belgium) in a dark room using a digital screen (DELL, U2412Mb, Limerick, Ireland). The images were evaluated by two examiners (NA, MA) according to the criteria previously prescribed<sup>23</sup> using the scale of E<sub>0</sub> to D<sub>2</sub> (Table I). For each specimen, the image with the deepest lesion was considered for score determination. In case of disagreement, the two examiners performed the examination again until consensus agreement was achieved.

### MODEL ASSEMBLING

After initial  $\mu$ -CT examination, carious teeth with lesion extension into the inner two-thirds of dentin (D<sub>2</sub> lesions) were excluded. Also, cracked teeth and teeth with obvious fluorosis were excluded. Eventually, in addition to the twelve sound teeth, twenty-seven carious teeth were selected for the main examination and for training and calibration sessions. Figure 6 illustrates samples distribution after model assembling.

For the main examination, thirty extracted premolars were selected based on lesion depth extension according to  $\mu$ -CT. The distribution was as follows: sound surface (E<sub>0</sub>: n=12); lesion in the outer half of the enamel (E<sub>1</sub>: n=6); lesion in the inner half of the enamel (E<sub>2</sub>: n=6); lesion in the outer one-third of the dentin (D<sub>1</sub>: n=6).

Three of the twelve sound teeth used for the main examination were also used for training and calibration. Furthermore, additional nine carious teeth (not included in the main examination) were selected for training and calibration. The distribution of the teeth for training and calibration was as follows: sound surface (E<sub>0</sub>: n=3), lesion in the outer half of the enamel (E<sub>1</sub>: n=3), lesion in the inner half of the enamel (E<sub>2</sub>: n=3), lesion in the outer one-third of the dentin (D<sub>1</sub>: n=3).

For each specimen, the apical one-third of the root was reduced using diamond discs (Lapcraft's L'il Trimmer™, Powell, Ohio, USA), leaving the coronal two-thirds of the root. The teeth were mounted on Lego® plastic bricks (The LEGO Group, Billund, Denmark) with the test surface adjacent to a sound tooth. The height of contact, lesion and marginal ridge were standardized at the same level for all specimens. Triad® visible light cure resin (DENTSPLY International, Inc., York, PA, USA) was applied around the root and the cervical part of the teeth at the level of the cemento-enamel junction resembling the anatomy of the gingiva. The selection of triad® visible light cure resin was based on a pilot study. Several extracted premolars were mounted using different imbedding materials. NIDIT Images were acquired and evaluated in order to obtain images with contrast comparable with *in-vivo* NIDIT images available in public sources.<sup>58, 59, 154, 155</sup> Dental floss was used to confirm the presence of the approximal contact (Figure 7). The assembled models were kept in a sealed plastic container with wet gauze to maintain humidity.

#### MAIN M-CT IMAGE ACQUISITION

After model assembling, the eighteen carious teeth selected for the main examination were scanned using  $\mu$ -CT in the same manner described previously in the “Initial Microfocus Computed Tomography ( $\mu$ -CT) Image Acquisition” section.

#### DIGITAL RADIOGRAPHY (DR) IMAGE ACQUISITION

The mounted teeth were placed on a custom film holder with a beam-aiming device (Figure 8). The DR images were obtained using Schick 33 CDR sensor (Sirona Dental Inc., Long Island City, NY, USA) at 60kV, 7 mA/ 0.20 seconds (Sirona, Heliodent DS. Bensheim, Germany). Plexiglass, 10×2.5×10 cm, was placed to simulate

the soft tissue effect between the x-ray tube head and the tooth (Figure 8.) The images were saved using dedicated software (CDR<sup>®</sup> DICOM, Schick Technologies Inc., Long Island City, NY). The images were extracted and stored in uncompressed TIFF format.

#### Digital Imaging Fiber Optic Transillumination (DIFOTI) Image Acquisition

An investigator (NA), who did not participate in DIFOTI examinations, obtained the images under standard conditions. The DIFOTI instrument (Electro-Optical Sciences Inc., Irvington, NY) was used to transilluminate the teeth to acquire the images and display them on the monitor. The images were obtained after air-drying in a dark room using two types of mouthpieces. The occlusal mouthpiece was used to transilluminate the tooth with a visible white light in a direction parallel to the CCD camera to obtain the occlusal image (DIFOTI-Occlusal). The approximal mouthpiece was used to transilluminate the tooth in a direction perpendicular to the CCD sensor to obtain the axial (buccal and lingual) images (DIFOTI-Buccal, DIFOTI-Lingual) (Figure 9). A dedicated DIFOTI program (DIFOTI version 2, Electro-Optical Sciences Inc., Irvington, NY, USA) was used to save and display the images.

#### TRAINING AND CALIBRATION

Three examiners (MA, AH, AG) who had more than 10 years of clinical teaching and research experience were trained on ICDAS, DR, DIFOTI and NIDIT examinations, prior to the main examination. The training course included theoretical elements in a PowerPoint presentation for one hour, and hands-on training on the previously obtained specimens for ICDAS and NIDIT, DR and DIFOTI images for three hours. Nine out of

the twelve calibration samples prescribed in “Model Assembling” were used for the hands-on training.

Prior to the calibration session, a project manual (Appendix) was distributed to the examiners with full instructions for each examination. The examiners performed the examination during separate sessions. NA randomly ordered the samples between examiners and before each examination using the random function of Microsoft Excel software (Microsoft® Excel® version 14.6.0, Microsoft Corporation, Redmond, WA, USA).

#### ICDAS CALIBRATION

The samples were placed on a tabletop just above knee level of the examiners. The examiners were instructed to sit in an upright position and to have no direct access to the approximal surfaces. The ICDAS examination was performed under a dental light unit, using a ball-ended probe and air-water syringe. Each specimen was removed from a container with 100-percent humidity, examined, air dried up to 5 seconds and examined again. The examiners used a mouth mirror to examine from the buccal and the lingual sides. The test approximal surface of each specimen was examined and the highest score from 0 to 4 was recorded according to ICDAS-II (Table II).<sup>26</sup>

#### DR CALIBRATION

The images were displayed randomly on a digital screen in a dark room (DELL, U2412Mb, Limerick, Ireland) via image viewer software (Windows Photo Viewer, version Windows 7, Microsoft, Redmond, WA). The images were evaluated by the three examiners according to the criteria previously prescribed<sup>23</sup> using the scale of E<sub>0</sub> to D<sub>1</sub> (Table III).

## DIFOTI CALIBRATION

The images were displayed randomly in a dark room on a digital screen via dedicated DIFOTI software (Electro-Optical Sciences Inc., Irvington, NY). The occlusal image (DIFOTI-Occlusal) was viewed and scored first for presence of approximal caries, followed by buccal and lingual images (DIFOTI-Buccal, DIFOTI-Lingual). Each approximal surface was scored for presence of shadowing as a caries lesion according to previously described criteria (Table IV).<sup>156, 157</sup>

## NIDIT CALIBRATION

After air-drying, each specimen was examined with NIDIT (CariVu™, DEXIS, LLC, Hatfield, PA) in a dark room. The examiners were instructed to place the light aperture and make it contact the gingiva; the NIDIT camera was centered perpendicularly over the test tooth. The live picture was monitored on the digital screen (DELL, U2412Mb, Limerick Ireland) and when the examiners were satisfied with the captured image, they were asked to save it and report the score. The images were captured and saved through the software (DEXIS, version 9.4.0, Hatfield, PA). The scoring criteria are described in Table V.

## REPEATED CALIBRATION

Each examiner performed ICDAS, DR, DIFOTI, and NIDIT calibration again at least two days after the initial calibration and in the same manner as previously described.

## STATISTICAL ANALYSIS AFTER CALIBRATION

Intra-examiner repeatability and inter-examiner agreement of all methods were assessed using intraclass correlation coefficients (ICCs). Two-way tables were also used to provide additional information about the repeatability and agreement.

## CALIBRATION RESULTS

The intra-examiner repeatability-ICCs after calibration were as follows: ICDAS (0.58), DR (0.86), NIDIT (0.71), DIFOTI-Occlusal (0.53), DIFOTI-Buccal (0.92), and DIFOTI-Lingual (0.85). The inter-examiner agreement-ICCs were as follows: ICDAS (0.58), DR (0.86), NIDIT (0.71), DIFOTI-Occlusal (0.53), DIFOTI-Buccal (0.92), and DIFOTI-Lingual (0.83).

The repeatability and agreement were not satisfactory except for DR, DIFOTI-Buccal and DIFOTI-Lingual. Therefore, the training and calibration of all methods except DR were performed again as previously described. The intra-examiner repeatability-ICCs were as follows: ICDAS (0.49), NIDIT (0.81), DIFOTI-Occlusal (0.87), DIFOTI-Buccal (0.87), DIFOTI-Lingual (0.83). The inter-examiner agreement-ICCs were as follows: ICDAS (0.48), NIDIT (0.81), DIFOTI-Occlusal (0.87), DIFOTI-Buccal (0.86), DIFOTI-Lingual (0.83).

## MAIN EXAMINATIONS

### ICDAS MAIN EXAMINATION

The examiners performed ICDAS examination in the same manner as described in the “ICDAS Calibration.” Repeated ICDAS examination was performed one week after main examination.

## DR MAIN EXAMINATION

The examiners performed DR examination in the same manner as described in the “DR Calibration.” Repeated DR examination was performed one week after main examination.

## DIFOTI MAIN EXAMINATION

The examiners performed DIFOTI examination in the same manner as described in the “DIFOTI calibration.” Repeated DIFOTI examination was performed one week after main examination.

## NIDIT MAIN EXAMINATION

The examiners performed NIDIT examination in the same manner as described in the “NIDIT calibration.” Repeated NIDIT examination was performed one week after main examination.

## SAMPLE SIZE JUSTIFICATION

Data from previous studies indicated a correlation of approximately 0.7 between methods. With a sample size of 10 sound teeth and 5 teeth for each of E<sub>1</sub>, E<sub>2</sub>, and D<sub>1</sub>, the study had an 80% power to detect a difference in the area under receiver operating characteristic (ROC) curve of 0.23 (0.67 vs. 0.90), assuming a two-sided test with a 5% significance level.

## STATISTICAL ANALYSIS

DIFOTI was assessed using three views – occlusal, buccal, and lingual. The maximum among the three views was used for the analyses labeled as DIFOTI, only the

occlusal view was used for DIFOTI-Occlusal, and the maximum of the DIFOTI-Buccal and DIFOTI-Lingual views was used for the analyses labeled as DIFOTI-BL.

Intra-examiner repeatability and inter-examiner agreement of all methods were assessed using intraclass correlation coefficients (ICCs). Two-way tables were also used to provide additional information about the repeatability and agreement.

Comparisons among the ICDAS, Digital Radiography, DIFOTI, and NIDIT methods for sensitivity (Sn), specificity (Sp), and area under the receiver operating characteristic (ROC) curves ( $A_z$ ) were performed using bootstrap analyses. The correlations among the measurements and the correlations of the measurements with the  $\mu$ -CT were also calculated using bootstrap methods.



## RESULTS

A total of 30 approximal sites were examined. Based on the  $\mu$ -CT gold standard, 12 teeth were sound ( $E_0$ ); six teeth exhibited lesion depth extension in the outer half of the enamel ( $E_1$ ); six teeth had lesion depth extension in the inner half of the enamel ( $E_2$ ), and six teeth had lesion depth extension in the outer one-third of the dentin ( $D_1$ ).

The intra-examiner repeatability and inter-examiner agreements are presented in Table VI and Figure 10. Intraclass correlation coefficients (ICCs), values of the intra-examiner repeatability, and inter-examiner agreements were interpreted based on Landis and Koch.<sup>158</sup> The repeatability and agreement were almost perfect for DIFOTI, substantial for ICDAS and NIDIT, and moderate for DR.

Overall sensitivity ( $S_n$ ), specificity ( $S_p$ ), and area under the ROC curve ( $A_z$ ) for DIFOTI, DR, ICDAS, and NIDIT are presented in Table VII.  $S_n$  and  $S_p$  are presented in Figure 11. The  $S_n$  was significantly lower for DR than for DIFOTI ( $p = 0.003$ ), DIFOTI-BL ( $p = 0.017$ ), and ICDAS ( $p = 0.006$ ). The  $S_n$  of DR was not significantly different from NIDIT ( $p = 0.251$ ). The  $S_n$  was significantly lower for NIDIT than for DIFOTI ( $p = 0.028$ ) and ICDAS ( $p = 0.049$ ), but was not significantly different from DIFOTI-BL ( $p = 0.0142$ ). The  $S_n$  was not significantly different between DIFOTI and ICDAS ( $p = 0.827$ ). The  $S_p$  was not significantly different among the methods (all  $p > 0.05$ ).

For  $\mu$ -CT =  $E_1$  (Figure 12, Table VII),  $S_n$  was significantly lower for DIFOTI-Occlusal than for DIFOTI ( $p = 0.001$ ), DIFOTI-BL ( $p = 0.010$ ), ICDAS ( $p < 0.001$ ), and NIDIT ( $p = 0.044$ ). No other significant differences in  $S_n$  were found among the methods

(all  $p > 0.12$ ). For  $\mu$ -CT = E<sub>2</sub>, Sn was significantly lower for DIFOTI-Occlusal than for DIFOTI ( $p = 0.025$ ). No other significant differences in Sn were found among the methods ( $p > 0.06$ ). For  $\mu$ -CT = D<sub>1</sub>, Sn was significantly lower for DR than for DIFOTI ( $p = 0.010$ ), DIFOTI-BL ( $p = 0.029$ ), and ICDAS ( $p = 0.019$ ). No other significant differences in Sn were found among the methods ( $p > 0.06$ ).

Area under the ROC curve ( $A_z$ ) (Figure 13 and Table VII) was significantly lower for DIFOTI-Occlusal than for DIFOTI ( $p < 0.001$ ), DIFOTI-BL ( $p < 0.001$ ), ICDAS ( $p = 0.001$ ), and NIDIT ( $p = 0.034$ ), but was not different from DR ( $p = 0.915$ ).  $A_z$  was significantly lower for DR than for DIFOTI ( $p = 0.002$ ), DIFOTI-BL ( $p = 0.001$ ), and ICDAS ( $p = 0.005$ ) but was not different from NIDIT ( $p = 0.052$ ). DIFOTI, DIFOTI-BL, ICDAS, and NIDIT were not significantly different from each other ( $p > 0.12$ ).

For correlations between the methods (DIFOTI, DR, ICDAS, and NIDIT) and  $\mu$ -CT (Table VIII and Figure 14), DIFOTI (correlation = 0.79,  $p < 0.001$ ), DIFOTI-BL (correlation = 0.80,  $p < 0.001$ ), ICDAS (correlation = 0.74,  $p < 0.001$ ), and NIDIT (correlation = 0.65,  $p < 0.001$ ) were moderately associated. DIFOTI-Occlusal was weakly associated with  $\mu$ -CT (correlation = 0.39,  $p = 0.028$ ). DR was not associated with  $\mu$ -CT (correlation = 0.19,  $p = 0.289$ ).

FIGURES AND TABLES

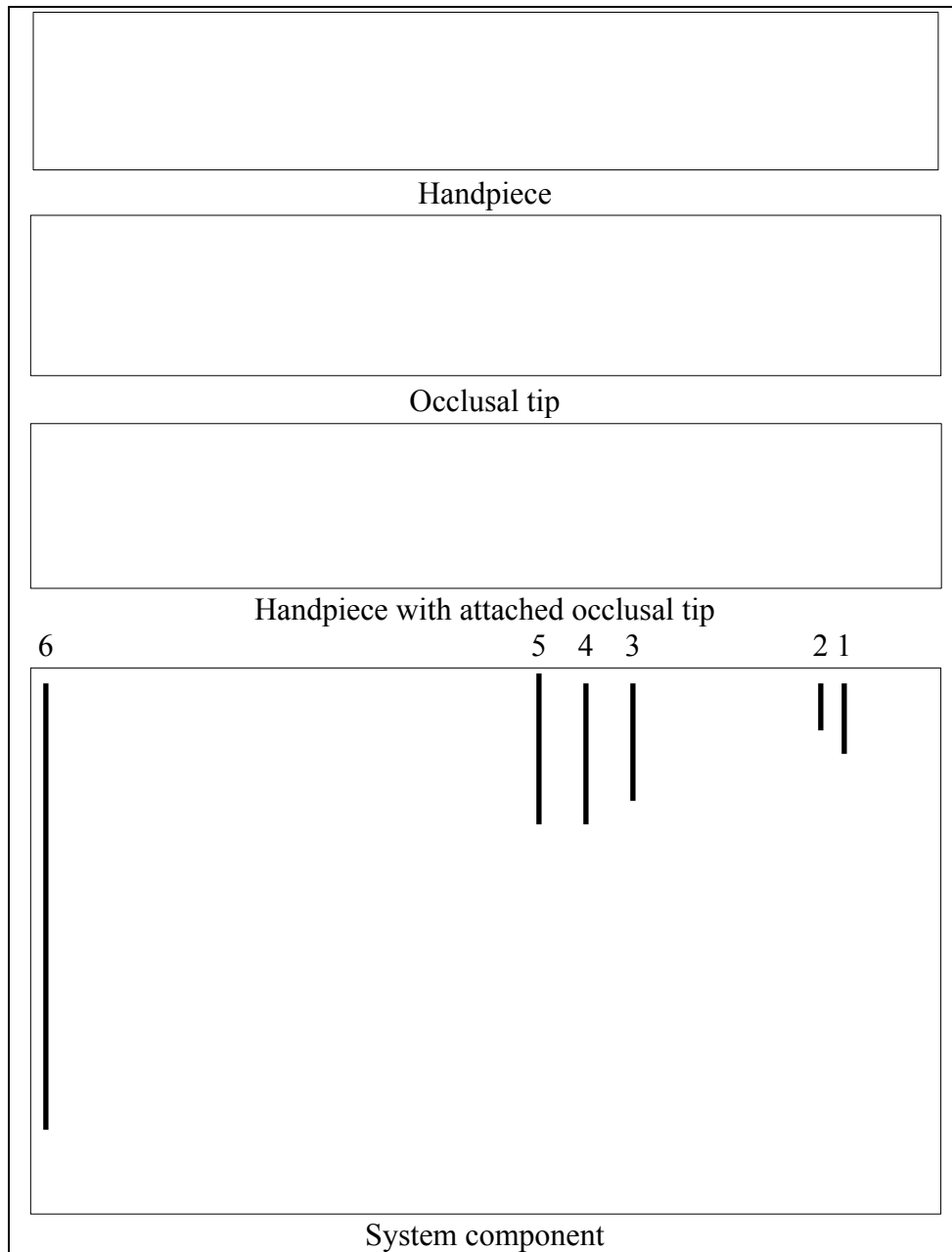


FIGURE 1. Near Infrared Digital Imaging Transillumination (NIDIT) Device System Components.

1	Aperture for laser beam	2	Opening for camera window
3	Ring Switch	4	Control Button 1
5	Control Button 2	6	USB cable to connect to computer

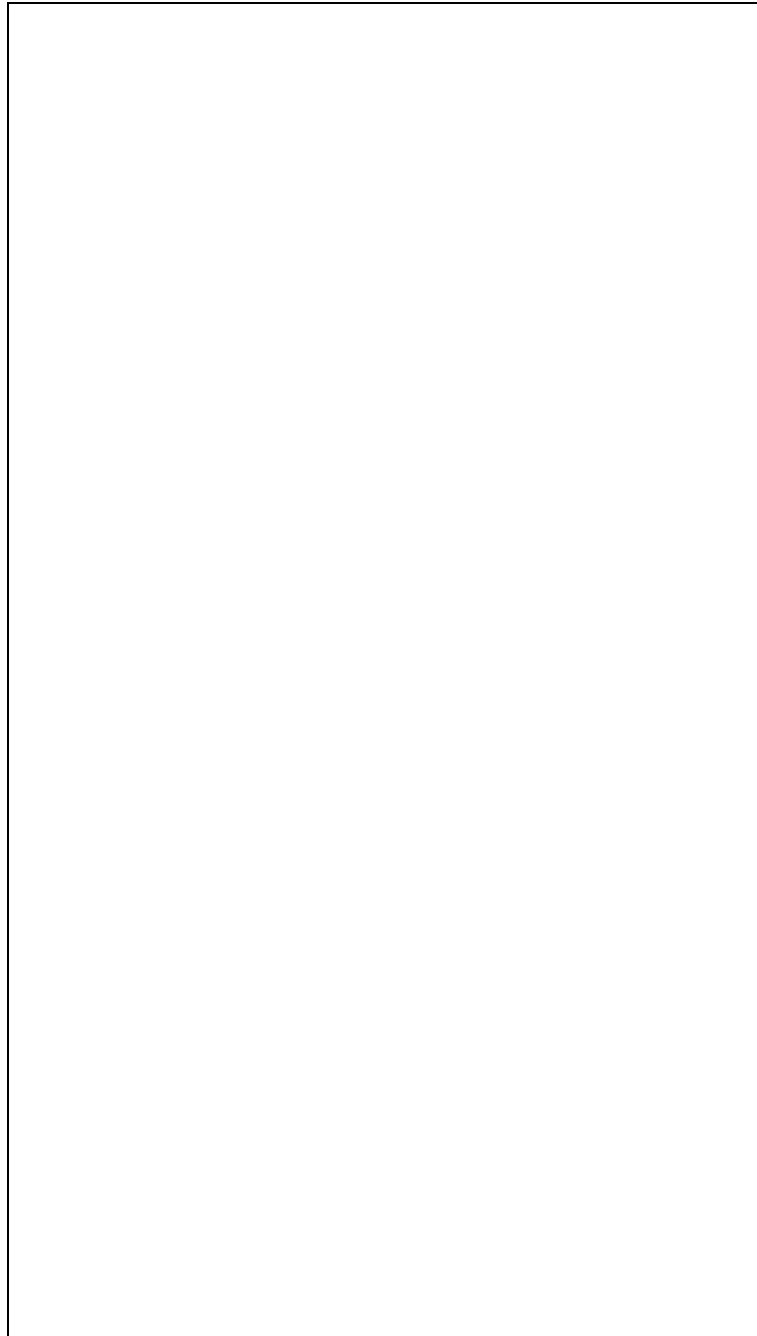


FIGURE 2. a. Schematic illustration of Near Infrared Digital Imaging Transillumination (NIDIT). (1) Elastic arms. (2) NIDIT light source.  
b. Illustration of NIDIT tip position for image acquisition.

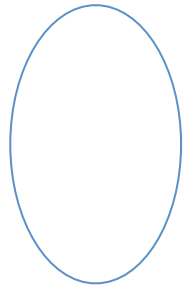


FIGURE 3. Near Infrared Digital Imaging Transillumination image of a premolar with approximal caries lesion. The blue circle indicates the caries lesion.

Teeth Selection

Initial Microfocus Computed Tomography ( $\mu$ -CT) Image  
Acquisition for lesion depth evaluation

Model Assembling

Main  $\mu$ -CT Image Acquisition to establish gold standard

Training

Calibration

Repeated Calibration

Statistical Analysis after Calibration

Main Examination

Repeated Examination

Statistical Analysis

FIGURE 4. Flow chart of the study



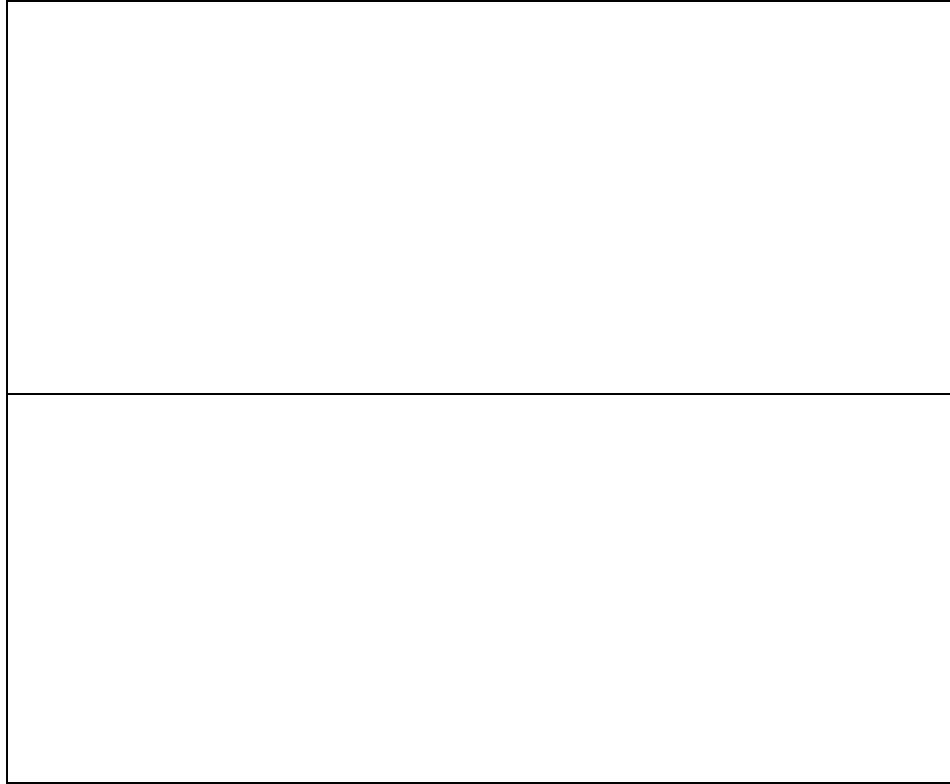


FIGURE 5. a). Skyscan 1172 high-resolution microfocus computed tomography machine. b). Tooth sample in rotating stage inside scanning chamber.

FIGURE 6. Sample distribution flow chart.

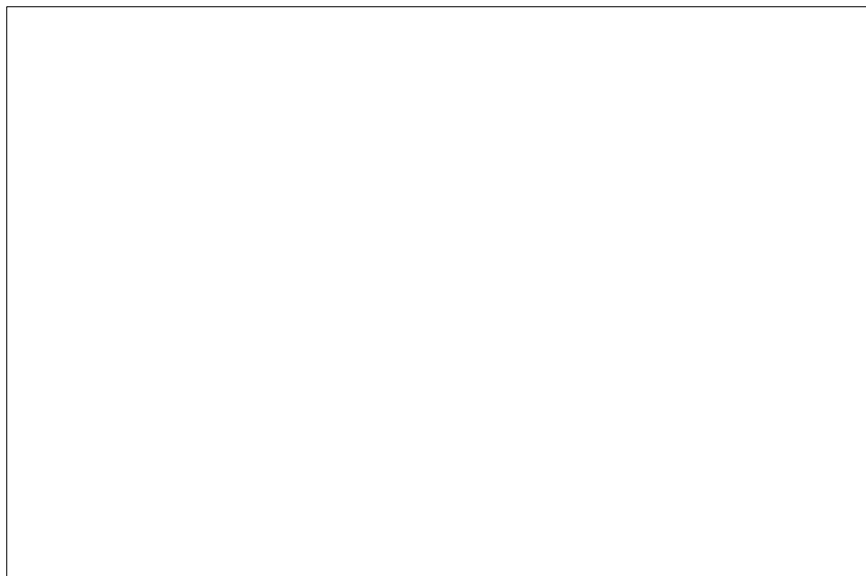


FIGURE 7. Sample assembly on Lego<sup>®</sup> bricks.



FIGURE 8. a) Custom film holder with beam aiming device and X-ray tube positioning. b) Main components for digital radiography image acquisition. 1) X-ray tube head. 2) Plexiglass. 3) Assembled teeth. 4) X-ray sensor.

	Occlusal View	Buccal View	Lingual View
Sound approximal surface			
Carious approximal surface			

FIGURE 9. Digital Imaging Fiber Optic Transillumination (DIFOTI) images acquisition. The blue circles indicate the examined sites.

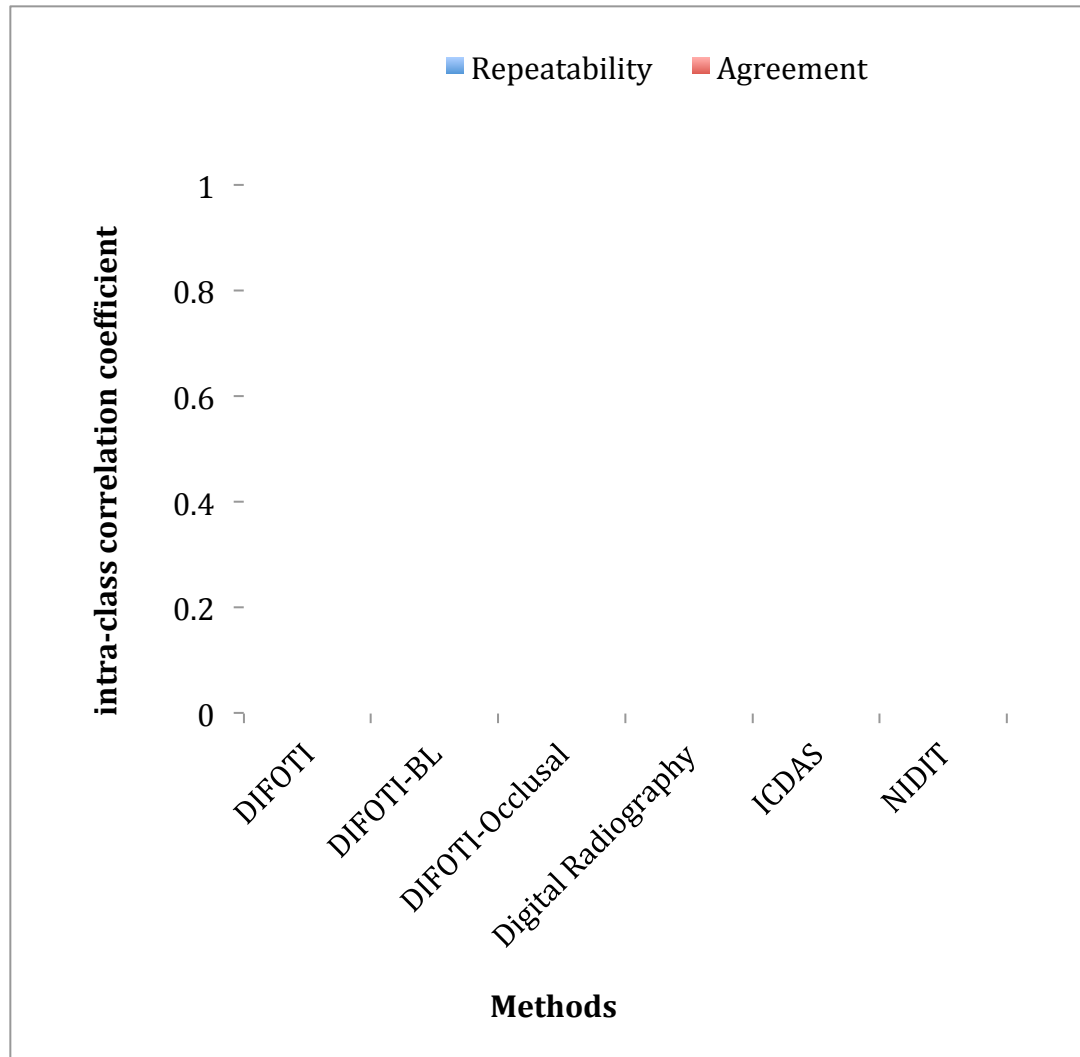


FIGURE 10. Intra-examiner repeatability and inter-examiner agreements using intra-class correlation coefficient from three examiners.

DIFOTI = Digital Imaging Fiber Optic Transillumination.

DIFOTI-BL = Digital Imaging Fiber Optic Transillumination from and lingual views.

DIFOTI-Occlusal = Digital Imaging Fiber Optic Transillumination from occlusal.

ICDAS = International Caries Detection and Assessment System.

NIDIT = Near Infrared Digital Imaging Transillumination.

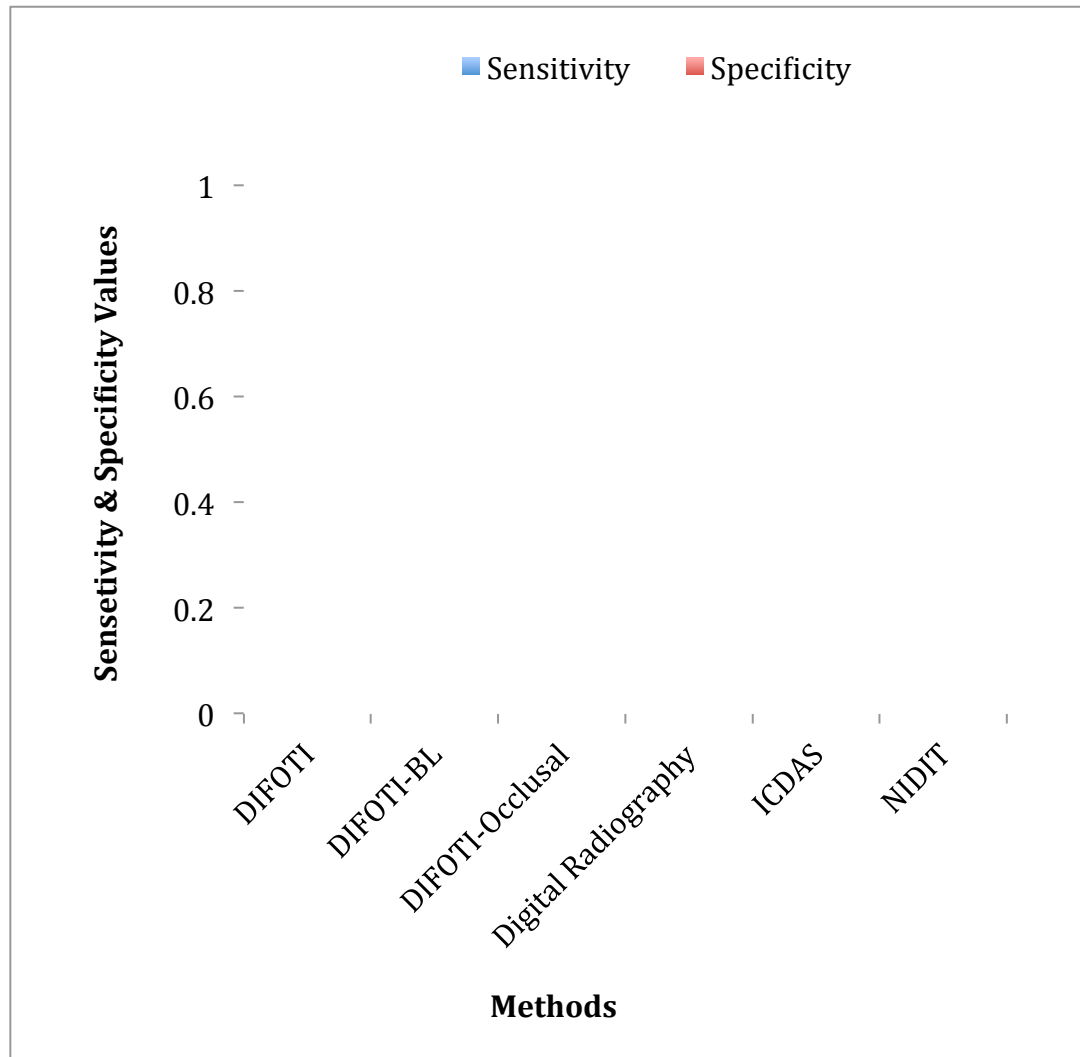


FIGURE 11. Overall sensitivity and specificity of caries detection methods.

DIFOTI = Digital Imaging Fiber Optic Transillumination.

DIFOTI-BL = Digital Imaging Fiber Optic Transillumination from buccal and lingual views.

DIFOTI-Occlusal = Digital Imaging Fiber Optic Transillumination from occlusal.

ICDAS = International Caries Detection and Assessment System.

NIDIT = Near Infrared Digital Imaging Transillumination.

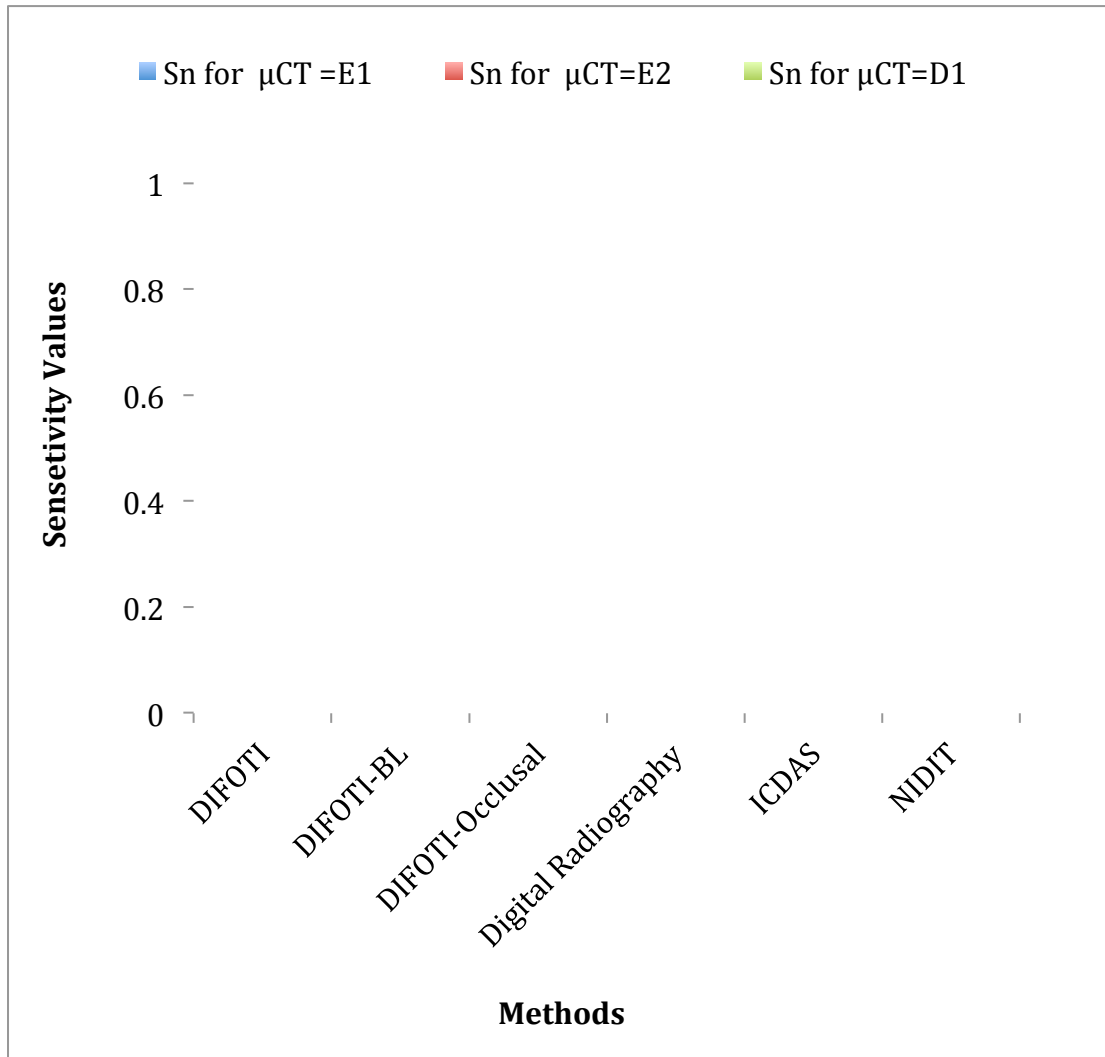


FIGURE 12. Sensitivity of caries detection methods at three caries depth thresholds.  $\mu$ CT= Microfocus computed tomography.

E<sub>1</sub>= lesion in the outer half of enamel.

E<sub>2</sub>= Lesion in the inner half of enamel.

D<sub>1</sub>=lesion in the outer one-third of dentin.

DIFOTI = Digital Imaging Fiber Optic Transillumination.

DIFOTI-BL = Digital Imaging Fiber Optic Transillumination from buccal and lingual views.

DIFOTI-Occlusal = Digital Imaging Fiber Optic Transillumination from occlusal.

ICDAS = International Caries Detection and Assessment System.

NIDIT = Near Infrared Digital Imaging Transillumination.



FIGURE 13. Receiver operating characteristic curves.

DIFOTI = Digital Imaging Fiber Optic Transillumination.

DIFOTI-BL = Digital Imaging Fiber Optic Transillumination from buccal and lingual views.

DIFOTI-Occlusal = Digital Imaging Fiber Optic Transillumination from occlusal.

ICDAS = International Caries Detection and Assessment System.

NIDIT = Near Infrared Digital Imaging Transillumination.

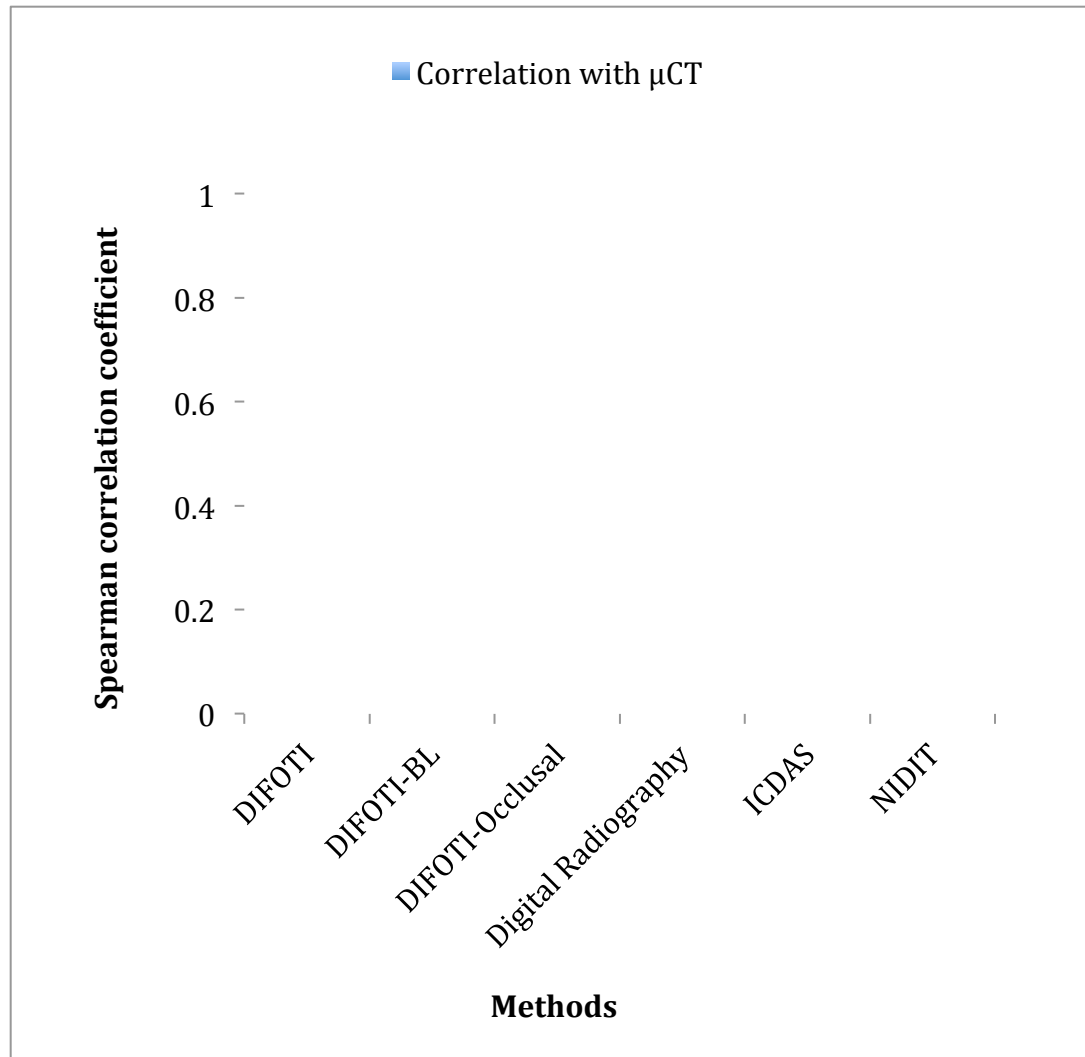


FIGURE 14. Spearman correlation coefficient of the detection methods with micro focus computed tomography ( $\mu$ CT).

DIFOTI = Digital Imaging Fiber Optic Transillumination.

DIFOTI-BL = Digital Imaging Fiber Optic Transillumination from buccal and lingual views.

DIFOTI-Occlusal = Digital Imaging Fiber Optic Transillumination from occlusal.

ICDAS = International Caries Detection and Assessment System.

NIDIT = Near Infrared Digital Imaging Transillumination.

TABLE I

Microfocus computed tomography ( $\mu$ -CT) scoring criteria

Score	Image	Criterion
E <sub>0</sub>		No radiolucency present.
E <sub>1</sub>		Radiolucency extends to the outer half of the enamel.
E <sub>2</sub>		Radiolucency extends to the inner half of the enamel and does not extend beyond the DEJ.
D <sub>1</sub>		Radiolucency extends to the outer one-third of the dentin.
D <sub>2</sub>		Radiolucency extends to the inner two-thirds of the dentin.

TABLE II

International Caries Detection and Assessment System, ICDAS-II scoring criteria

Score	Criterion	Image
0	No evidence of visible caries when viewed clean and after prolonged air-drying (5 seconds). Surfaces with developmental defects such as enamel hypomineralization (including fluorosis); tooth wear (attrition, abrasion and erosion), and extrinsic or intrinsic stains were recorded as sound.	
1	Opacity or discoloration not visible on wet surface, but distinctly visible after 5 seconds of air-drying. Usually seen from lingual/buccal or from occlusal.	
2	Opacity or discoloration distinctly visible on wet surface. Usually seen from lingual/ buccal or from occlusal as a shadow confined to enamel.	
3	Caries loss of enamel integrity viewed from buccal and lingual direction. Confirmation can be assisted with use of explorer gently across the surface to confirm enamel micro-cavity/discontinuity.	
4	It appears as a shadow of grey, blue or brown discolored dentin. Directly seen from lingual /buccal and when a discolored dentin is visible through the occlusal marginal ridge.	

TABLE III  
Radiography scoring criteria

Score	Image	Criterion
E <sub>0</sub>		No radiolucency present.
E <sub>1</sub>		Radiolucency extends to the outer half of the enamel.
E <sub>2</sub>		Radiolucency extends to the inner half of the enamel and does not extend beyond the dentino-enamel junction (DEJ).
D <sub>1</sub>		Radiolucency extends to the outer one-third of the dentin.

TABLE IV

Digital imaging fiber optic transillumination scoring criteria

Score	Criterion
0	No caries
1	Probably no caries present
2	Not sure
3	Probably caries is present
4	Caries present

TABLE V

Scoring criteria for near infrared digital imaging transillumination

Score	Image	Criterion
E <sub>0</sub>		No shadowing.
E <sub>1</sub>		Shadow in outer half of enamel.
E <sub>2</sub>		Shadow in inner half of enamel, but not to dentino-enamel junction (DEJ).
D <sub>1</sub>		Shadow extended to DEJ, but not beyond outer one third of dentin.

TABLE VI

Intra-examiner repeatability and inter-examiner agreements using ICC

Method	Repeatability				Agreements
	All	Examiner 1	Examiner 2	Examiner 3	
DIFOTI	0.85	0.83	0.87	0.86	0.83
DIFOTI-BL	0.92	0.93	0.98	0.86	0.89
DIFOTI-Occlusal	0.64	0.66	0.67	0.71	0.58
Digital Radiography	0.52	0.44	0.62	0.67	0.48
ICDAS	0.79	0.69	0.90	0.83	0.72
NIDIT	0.69	0.78	0.80	0.59	0.64

DIFOTI = Digital Imaging Fiber Optic Transillumination.

DIFOTI-BL = Digital Imaging Fiber Optic Transillumination from buccal and lingual views.

DIFOTI-Occlusal = Digital Imaging Fiber Optic Transillumination from occlusal.

ICDAS = International Caries Detection and Assessment System.

NIDIT = Near Infrared Digital Imaging Transillumination.

---



TABLE VII

Specificity, sensitivity, area under Receiver Operating Characteristic curve

Method	Sn	Sp	Sn for $\mu\text{CT} = \text{E}_1$	Sn for $\mu\text{CT} = \text{E}_2$	Sn for $\mu\text{CT} = \text{D}_1$	$A_z$
DIFOTI	0.91 <sup>a</sup>	0.69	0.72 <sup>a</sup>	1.00 <sup>a</sup>	1.00 <sup>a</sup>	0.91 <sup>a</sup>
DIFOTI-BL	0.86 <sup>a,b</sup>	0.93	0.69 <sup>a</sup>	0.92 <sup>a,b</sup>	0.97 <sup>a</sup>	0.92 <sup>a</sup>
DIFOTI-Occlusal	0.42 <sup>c</sup>	0.75	0.03 <sup>b</sup>	0.50 <sup>b</sup>	0.72 <sup>a,b</sup>	0.60 <sup>c</sup>
Digital Radiography	0.50 <sup>c</sup>	0.64	0.39 <sup>a,b</sup>	0.67 <sup>a,b</sup>	0.44 <sup>b</sup>	0.61 <sup>b,c</sup>
ICDAS	0.89 <sup>a</sup>	0.83	0.81 <sup>a</sup>	0.92 <sup>a,b</sup>	0.94 <sup>a</sup>	0.90 <sup>a</sup>
NIDIT	0.68 <sup>b,c</sup>	0.93	0.50 <sup>a</sup>	0.61 <sup>a,b</sup>	0.92 <sup>a,b</sup>	0.81 <sup>a,b</sup>

Sn = Sensitivity.

Sp = Specificity.

$A_z$  = Area under Receiver Operating Characteristic (ROC) curve.

$\mu\text{CT}$  = Microfocus computed tomography.

$\text{E}_1$  = lesion in the outer half of enamel.

$\text{E}_2$  = Lesion in the inner half of enamel.

$\text{D}_1$  = lesion in the outer one-third of dentin.

DIFOTI = Digital Imaging Fiber Optic Transillumination.

DIFOTI-BL = Digital Imaging Fiber Optic Transillumination from buccal and lingual views.

DIFOTI-Occlusal = Digital Imaging Fiber Optic Transillumination from occlusal.

ICDAS = International Caries Detection and Assessment System.

NIDIT = Near Infrared Digital Imaging Transillumination.

Within column, same superscript letters indicate no significant differences.

TABLE VIII  
Spearman correlation coefficient of the methods

Method	Correlation with $\mu$ CT	P value
DIFOTI	0.79	$p < 0.001$
DIFOTI-BL	0.80	$p < 0.001$
DIFOTI-Occlusal	0.39	$p = 0.028$
Digital Radiography	0.19	$p = 0.289$
ICDAS	0.74	$p < 0.001$
NIDIT	0.65	$p < 0.001$

DIFOTI = Digital Imaging Fiber Optic Transillumination.

DIFOTI-BL = Digital Imaging Fiber Optic Transillumination from buccal and lingual views.

DIFOTI-Occlusal = Digital Imaging Fiber Optic Transillumination from occlusal.

ICDAS = International Caries Detection and Assessment System.

NIDIT = Near Infrared Digital Imaging Transillumination.

$\mu$ CT = Microfocus computed tomography.

---

DISCUSSION

Dental caries is a dynamic process. As de- and remineralization of tooth structure occurs over time, such that the net balance of these events will determine the rate of lesion progression to a state that can be detected by any means of caries detection methodologies.<sup>1-5</sup> When dental caries is detected before surface cavitation occurs, preventive therapy can arrest the progression of active caries lesions before they reach to cavitation stage.<sup>159</sup> This treatment approach requires valid as well as reliable early caries detection methods in order to successfully detect and monitor the change in lesion progression, especially at non-cavitated stages.<sup>5, 160</sup>

Approximal caries detection is a difficult task for clinicians mainly because of the presence of the contact with neighboring teeth, which limits direct visual access of the unaided eyes.<sup>161</sup> Radiography is traditionally used, as it can show signs of demineralization of clinically inaccessible surfaces.<sup>16-18, 34</sup> However, methods based on optical observation of approximal surfaces are improving and it appears that methods based on light transillumination can detect lesions at early stages.<sup>56, 84</sup>

Regarding the Near Infrared Digital Imaging Transillumination (NIDIT), the available scientific data are limited. Kuhnisch et al.<sup>59</sup> performed an *in-vivo* study to evaluate the performance of NIDIT. They compared the performance of NIDIT with bitewing radiography, laser fluorescence, and visual examination for detection of dentin-involved approximal caries. The reference standard was established after clinical caries excavation using radiography for lesion depth measurement. For this current study,

sensitivity (Sn) values at dentin threshold were agreed with Kuhnisch et al.<sup>59</sup> However, one of the disadvantages of Kuhnisch et al.<sup>59</sup> study can be attributed to the unavoidable selection bias in any *in-vivo* diagnostic study. For ethical reasons, only teeth that showed visual and radiographic signs of dentin-involved approximal caries lesions were included in their sample.<sup>59</sup> Due to lacking of negative control, specificity (Sp) values could not be calculated. Our current *in-vitro* study was designed in order to evaluate the detection performance of this novel method.

Near infrared (NIR) light (wavelength: 700 nm to 2000 nm) can penetrate deeper enamel due to enamel's reduced scattering coefficient ( $\mu_s$ ) within NIR wavelength spectrum. The scattering coefficient of enamel in the visible wavelength is  $60 \text{ cm}^{-1}$  at 632 nm and decreases as the wavelength increases to the NIR spectrum ( $\mu_s = 2$  to  $3 \text{ cm}^{-1}$  at 1310 nm and 1550 nm).<sup>162, 163</sup> Fried et al.<sup>164</sup> demonstrated that when NIR light was delivered close to the cementoenamel junction, the approximal lesions could be viewed from the occlusal. This is because light with wavelength in the NIR range can penetrate deeper enamel thicknesses.<sup>162-164</sup> Staninec et al.<sup>165</sup> evaluated the performance of a prototype device that uses NIR light from buccal, lingual and occlusal views at 1310 nm for approximal caries detection *in vivo*. Thirty-three lesions were included based on bitewing radiography that served as the reference standard. NIR prototype device detected 32 lesions when all views (occlusal, buccal and lingual) were used to evaluate the approximal sites. NIR prototype device buccal and lingual views detected thirty lesions, while the occlusal view detected twenty-seven lesions.<sup>165</sup> This can be explained as the emitted light in NIR needed to travel through a large amount of surrounding enamel in order to reach the occlusal surface. The NIDIT manufacturer provides only

occlusal tips to acquire the images from the occlusal view. Development of an approximal tip allows imaging from the buccal and lingual view. This may improve NIDIT performance for approximal caries detection.

The performance of DIFOTI in this current study was in agreement with two previous *in-vitro* studies regarding sensitivity (Sn) and specificity (Sp), as well as the inter-examiner agreement and intra-examiner repeatability.<sup>56, 166</sup> However, previous studies did not clearly mention whether DIFOTI was used to detect lesions from occlusal or buccal and lingual views or a combination of all views. To the authors' knowledge, no information was found to demonstrate which view is more suitable to detect approximal caries. Our current study showed higher Sn and Sp values for DIFOTI-bucco-lingual (BL) than DIFOTI-Occlusal. A possible explanation is that DIFOTI relies on visible light (wavelength: 450 nm to 700 nm) to transilluminate the tooth. However, the wavelengths in the visible range (wavelength: 400 nm to 700 nm) are limited by strong light scattering by the tooth tissues, making it difficult to image through 1 mm to 2 mm thickness of tooth structure.<sup>167</sup> In DIFOTI-Occlusal view, the visibility of the early approximal lesion can be obscured by the presence of a sound marginal ridge, as the light needs to travel through a large amount of sound enamel. The results for this study illustrates that DIFOTI buccal and lingual view are more valid and reliable than DIFOTI occlusal views for early approximal caries detection.

In this current study, DIFOTI and NIDIT demonstrated that lesions involving the inner half of the enamel were more detectable than lesions in the outer half. This is in agreement with Ando's<sup>83</sup> observations regarding occlusal and smooth surface caries detection *in vivo* using DIFOTI. A possible explanation is that increased demineralization

may lead to increased light scattering and absorption.<sup>168</sup> This indicates the potential of light transillumination methods to quantify caries lesion.<sup>168</sup>

The superior performance of ICDAS, DIFOTI and NIDIT over DR could be attributed to the ability of the three former methods to detect early changes in the optical properties of demineralized enamel<sup>20</sup>; in contrast, a 30-percent to 40-percent mineral loss is necessary for the radiographic detection of enamel caries.<sup>169</sup> Furthermore, DR failed to show any association with  $\mu$ -CT depth scores, while NIDIT showed a moderate association. Radiographs usually underestimate the depth of the lesion. Location, shape and extent of the lesion, as well as the anatomy of the tooth, can influence radiographic depiction.<sup>16</sup> For example, superficial but widespread lesions across the approximal surface may appear as an overestimated deep lesion on a radiographic image, while deep but localized demineralization may appear as a shallow lesion.<sup>16</sup>

One of the disadvantages of NIDIT is that it cannot delineate the dental pulp because of the strong light scattering of the dentin.<sup>59</sup> Consequently, it is difficult to estimate the lesion depth in dentin in relation to the pulp. Therefore, the probability of approximal cavitation based on lesion depth cannot be estimated with the same confidence as in radiography.<sup>7</sup> Further study is needed to identify possible quantitative or qualitative indicators that can be used to determine or estimate dentin lesion depth.

Argument has been raised regarding the use of bitewing radiography for caries detection is justified and how long the intervals between radiographic examinations should be.<sup>55, 170</sup> The concern associated with bitewing radiography for caries detection is primarily due to the radiation risk and low sensitivity for detecting non-cavitated lesions.<sup>51, 52</sup> Therefore, it is still difficult to justify the repeated use of bitewing radiography to

detect lesions and consequently to evaluate the effectiveness of non-invasive preventive treatments.<sup>16, 19, 53-55</sup> One of the main advantages of NIDIT over radiography is the absence of ionizing radiation. Although the absorbed radiation dose from bitewing radiography is very low, further reduction or elimination of ionizing radiation is desirable.<sup>16, 19, 53-55</sup> The results of this *in-vitro* study demonstrated the potential of NIDIT for approximal non-cavitated caries detection. However, the performance of NIDIT for detection of early non-cavitated caries requires further *in-vivo* validation using a well-accepted gold standard (for example, *in-vitro* validation after primary tooth exfoliation).

Extrapolation of the results of this current *in-vitro* study should be considered very carefully. The main concern that may impact the clinical implication is the difficulty in simulating clinical approximal contacts. Although all examined approximal sites were in contact with adjacent teeth, the *in-vitro* assembling of the specimens may have produced smaller than “normal” contact points, leaving significant portions of the approximal surfaces visually accessible. Approximal point contacts are typically seen in younger patients.<sup>171</sup> However, within increase in age, the contact point become larger due to frictional wear of one approximal surface against another during physiologic movement of the teeth.<sup>171</sup> This will result in obscuring the approximal surface to direct visual access. Not surprisingly, *in-vitro* studies, including this current study, that evaluated ICDAS performance for early approximal caries detection<sup>31, 141</sup> showed significantly higher Sn values than typically reported in *in-vivo* studies<sup>30, 172, 173</sup> Another explanation for the better performance of ICDAS can be attributed to the examiners’ experience. It has been shown that the correct use of ICDAS-II and the examiner’s experience may improve the precision of visual examination.<sup>26, 174</sup>



A concern regarding an additional diagnostic yield is that it may lead to more false-positive diagnosis and consequently over-treatment, especially in populations regularly exposed to fluoride.<sup>16, 17</sup> However, the key for appropriate caries detection is found in the outcomes of caries diagnosis process. False positive diagnosis of an active non-cavitated caries lesion will not result in operative treatment, but in preventive non-surgical intervention, such as plaque control, topical fluoride and dietary modification. Although this means a cost to the patient, it does not result in a harmful health outcome. On the other hand, there are consequences of misdiagnose an active caries lesion. If the patient is caries-active with irregular dental visits, there is a risk of progression of non-cavitated lesion to cavitation before they are detected; thus requiring surgical intervention, such as restoration.<sup>175, 176</sup> However, if the patient has a low caries risk with regular dental visits, the lesion will probably be detected in a later visit before it progresses to the cavitation stage.<sup>138</sup>

In summary, although radiographic examination remains the most common method used to detect approximal caries lesions, our data suggest that radiography has less sensitivity than methods based on the optical properties of demineralized tooth structure. The results from NIDIT showed the potential of the method to serve as a useful non-irradiative method for approximal caries detection. ICDAS and DIFOTI presented higher validity and reliability than DR in this *in-vitro* study design.

SUMMARY AND CONCLUSION

For caries management, early detection of dental caries is an essential task. Early caries detection methods should be reliable and valid. Approximal caries detection remains a challenge for clinicians primarily because of the presence of the contact with a neighboring tooth. It limits direct visual access of the unaided eyes. Methods based on optical observation of approximal lesions are improving. It appears that methods based on light transillumination can detect lesions at early stages. Near Infrared Digital Imaging Transillumination (NIDIT) is a novel method that, to the authors' knowledge, no study has had evaluated its performance for early approximal caries detection. Our objectives were to evaluate the ability of NIDIT to detect non-cavitated enamel and dentin approximal caries lesions and to compare its performance to International Caries Detection and Assessment System (ICDAS), digital radiography (DR), and Digital Imaging Fiber Optic Transillumination (DIFOTI).

Thirty human extracted premolars were selected. The approximal surface status ranged from sound to surfaces with non-cavitated caries lesions into the outer one-third of the dentin. Lesion depth was determined by micro-computed tomography ( $\mu$ -CT) as a gold standard. Teeth were mounted in a custom-made device to simulate approximal contact. Three examiners were trained and calibrated. The intra-examiner repeatability and inter-examiner agreement of all methods were assessed using intraclass correlation coefficients (ICCs). ICDAS, DR, DIFOTI, and NIDIT examinations were performed and repeated. Sensitivity, specificity, area under ROC curve ( $A_z$ ), inter- and intra-class

correlation coefficients (ICCs) of each method, and correlation among the methods were determined.

ICCs for intra-/inter-examiner agreement were almost perfect for DIFOTI (0.85/0.83), substantial for ICDAS (0.79/0.72) and NIDIT (0.69/0.64), and moderate for DR (0.52/0.48). Sensitivity/specificity for DIFOTI, ICDAS, DR and NIDIT were 0.91/0.69, 0.89/0.83, 0.50/0.64, and 0.68/0.93, respectively. As for the comparison among the methods, Az of DR (0.61) was significantly lower than that of DIFOTI (0.91,  $p = 0.002$ ) and ICDAS (0.90,  $p = 0.005$ ), but was not significantly different from NIDIT (0.81,  $p = 0.052$ ). DIFOTI, ICDAS, and NIDIT were not significantly different from each other ( $p > 0.13$ ). Spearman correlation coefficients with  $\mu$ -CT for DIFOTI (0.79,  $p < 0.001$ ), ICDAS (0.74,  $p < 0.001$ ), and NIDIT (0.65,  $p < 0.001$ ) demonstrated a moderate association, while that of DR suggested no association (0.19,  $p = 0.289$ ).

Within the limitations of this *in-vitro* study, NIDIT system demonstrated a potential for early approximal caries detection. ICDAS, DIFOTI, and NIDIT were superior to DR in terms of validity and reliability. The encouraging results of NIDIT justify continuing investigation via an *in-vivo* model.

REFERENCES

1. Featherstone JD. Remineralization, the natural caries repair process--the need for new approaches. *Adv Dent Res* 2009;21(1):4-7.
2. Von der Fehr FR. The caries inhibiting effect of topically applied hexafluorostannate on dentine and enamel. *Caries Res* 1970;4(3):269-82.
3. Joyston-Bechal S, Kidd EA. The effect of three commercially available saliva substitutes on enamel in vitro. *Br Dent J* 1987;163(6):187-90.
4. Manji F, Fejerskov O, Nagelkerke NJ, Baelum V. A random effects model for some epidemiological features of dental caries. *Community Dent Oral Epidemiol* 1991;19(6):324-8.
5. Zero DT, Fontana M, Martinez-Mier EA, et al. The biology, prevention, diagnosis and treatment of dental caries: scientific advances in the United States. *J Am Dent Assoc* 2009;140 Suppl 1:25S-34S.
6. Beltran-Aguilar ED, Barker LK, Canto MT, et al. Surveillance for dental caries, dental sealants, tooth retention, edentulism, and enamel fluorosis--United States, 1988-1994 and 1999-2002. *MMWR Surveill Summ* 2005;54(3):1-43.
7. Pitts NB, Rimmer PA. An in vivo comparison of radiographic and directly assessed clinical caries status of posterior approximal surfaces in primary and permanent teeth. *Caries Res* 1992;26(2):146-52.
8. Kidd EA. The diagnosis and management of the 'early' carious lesion in permanent teeth. *Dent Update* 1984;11(2):69-70, 72-4, 76-8 passim.
9. O. Fejerskov, E.A.M. Kidd, Nyvad B, Baelum V. Defining the disease: an introduction. In: O. Fejerskov, Kidd EAM, editors. *Dental Caries the Disease and its Clinical Management*. 2nd ed. Oxford: Blackwell Munksgaard; 2008. p. 3-6.
10. Asmyhr O, Grytten L, Grytten J. Changing trends in caries experience among male military recruits in Norway. *Community Dent Oral Epidemiol* 1994;22(3):206-7.

11. Fure S, Zickert I. Incidence of tooth loss and dental caries in 60-, 70- and 80-year-old Swedish individuals. *Community Dent Oral Epidemiol* 1997;25(2):137-42.
12. Mejare I, Kallestal C, Stenlund H, Johansson H. Caries development from 11 to 22 years of age: a prospective radiographic study. Prevalence and distribution. *Caries Res* 1998;32(1):10-6.
13. Lith A, Pettersson LG, Grondahl HG. Radiographic study of approximal restorative treatment in children and adolescents in two Swedish communities differing in caries prevalence. *Community Dent Oral Epidemiol* 1995;23(4):211-6.
14. Mejare I, Stenlund H, Zelezny-Holmlund C. Caries incidence and lesion progression from adolescence to young adulthood: a prospective 15-year cohort study in Sweden. *Caries Res* 2004;38(2):130-41.
15. Martignon S, Chavarria N, Ekstrand KR. Caries status and proximal lesion behaviour during a 6-year period in young adult Danes: an epidemiological investigation. *Clin Oral Investig* 2010;14(4):383-90.
16. I. Mejare, Kidd EAM. Radiography for caries diagnosis. In: O. Fejerskov, E.A.M. Kidd, editors. *Dental Caries the Disease and its Clinical Management*. 2nd ed. Oxford: Blackwell Munksgaard; 2008. p. 69-88.
17. Wenzel A. Bitewing and digital bitewing radiography for detection of caries lesions. *J Dent Res* 2004;83 Spec No C:C72-5.
18. Pitts N. Advances in Radiographic Detection Methods and Caries Management Rationale Paper presented at: Early Detection of Dental Caries. Proceedings of the 1st Annual Indiana Conference 1996; Indiana University School of Dentistry
19. Bader JD, Shugars DA, Bonito AJ. A systematic review of the performance of methods for identifying carious lesions. *J Public Health Dent* 2002;62(4):201-13.
20. B. N, Fejerskov O, Baelum V. Visual-tactile caries diagnosis. In: Fejerskov O, Kidd EAM, editors. *Dental Caries the Disease and its Clinical Management*. 2nd ed. Oxford: Blackwell Munksgaard; 2008. p. 49-68.
21. Braga MM, Mendes FM, Ekstrand KR. Detection activity assessment and diagnosis of dental caries lesions. *Dent Clin North Am* 2010;54(3):479-93.

22. Ismail AI. Visual and visuo-tactile detection of dental caries. *J Dent Res* 2004;83 Spec No C:C56-66.
23. Ekstrand KR, Ricketts DN, Kidd EA. Reproducibility and accuracy of three methods for assessment of demineralization depth of the occlusal surface: an in vitro examination. *Caries Res* 1997;31(3):224-31.
24. Nyvad B, Machiulskiene V, Baelum V. Reliability of a new caries diagnostic system differentiating between active and inactive caries lesions. *Caries Res* 1999;33(4):252-60.
25. Fyffe HE, Deery C, Nugent ZJ, Nuttall NM, Pitts NB. In vitro validity of the Dundee Selectable Threshold Method for caries diagnosis (DSTM). *Community Dent Oral Epidemiol* 2000;28(1):52-8.
26. Ismail AI, Sohn W, Tellez M, et al. The International Caries Detection and Assessment System (ICDAS): an integrated system for measuring dental caries. *Community Dent Oral Epidemiol* 2007;35(3):170-8.
27. Ekstrand KR, Kuzmina I, Bjorndal L, Thylstrup A. Relationship between external and histologic features of progressive stages of caries in the occlusal fossa. *Caries Res* 1995;29(4):243-50.
28. Ismail A. Diagnostic levels in dental public health planning. *Caries Res* 2004;38(3):199-203.
29. Ekstrand KR, Luna LE, Promisiero L, et al. The reliability and accuracy of two methods for proximal caries detection and depth on directly visible proximal surfaces: an in vitro study. *Caries Res* 2011;45(2):93-9.
30. Gimenez T, Piovesan C, Braga MM, et al. Visual Inspection for Caries Detection: A Systematic Review and Meta-analysis. *J Dent Res* 2015;94(7):895-904.
31. Braga MM, Morais CC, Nakama RC, et al. In vitro performance of methods of approximal caries detection in primary molars. *Oral Surg Oral Med Oral Pathol Oral Radiol Endod* 2009;108(4):e35-41.
32. Bader JD, Shugars DA, Bonito AJ. Systematic reviews of selected dental caries diagnostic and management methods. *J Dent Educ* 2001;65(10):960-8.



33. Rindal DB, Gordan VV, Litaker MS, et al. Methods dentists use to diagnose primary caries lesions prior to restorative treatment: findings from The Dental PBRN. *J Dent* 2010;38(12):1027-32.
34. Gröndahl H-G. The value of radiologic examination in caries diagnosis. In: Thylstrup A, O Fejerskov, editors. *Textbook of clinical cariology* Copenhagen: Munksgaard; 1994. p. 376-82.
35. Schwendicke F, Tzschope M, Paris S. Radiographic caries detection: A systematic review and meta-analysis. *J Dent* 2015;43(8):924-33.
36. Bader JD, Shugars DA. Agreement among dentists' recommendations for restorative treatment. *J Dent Res* 1993;72(5):891-6.
37. Elderton RJ, Nuttall NM. Variation among dentists in planning treatment. *Br Dent J* 1983;154(7):201-6.
38. Pitts NB, Hamood SS, Longbottom C. Initial development and in vitro evaluation of the HPL device for obtaining reproducible bitewing radiographs of children. *Oral Surg Oral Med Oral Pathol* 1991;71(5):625-34.
39. van der Stelt PF, Ruttiman UE, Webber RL, Heemstra P. In vitro study into the influence of X-ray beam angulation on the detection of artificial caries defects on bitewing radiographs. *Caries Res* 1989;23(5):334-41.
40. Zappa U, Simona C, Graf H, van Aken J. In vivo determination of radiographic projection errors produced by a novel filmholder and an x-ray beam manipulator. *J Periodontol* 1991;62(11):674-83.
41. Okano T, Grondahl HG, Grondahl K, Webber RL. Effect of quantum noise on the detection of incipient proximal caries. *Oral Surg Oral Med Oral Pathol* 1982;53(2):212-8.
42. Kundel HL, Revesz G. Lesion conspicuity, structured noise, and film reader error. *AJR Am J Roentgenol* 1976;126(6):1233-8.
43. Revesz G, Kundel HL, Graber MA. The influence of structured noise on the detection of radiologic abnormalities. *Invest Radiol* 1974;9(6):479-86.

44. Matteson SR, Phillips C, Kantor ML, Leinedecker T. The effect of lesion size, restorative material, and film speed on the detection of recurrent caries. *Oral Surg Oral Med Oral Pathol* 1989;68(2):232-7.
45. Espelid I, Tveit AB. Diagnosis of secondary caries and crevices adjacent to amalgam. *Int Dent J* 1991;41(6):359-64.
46. Goshima T, Goshima Y. The optimum level of radiopacity in posterior composite resins. *Dentomaxillofac Radiol* 1989;18(1):19-21.
47. Hardison JD, Rafferty-Parker D, Mitchell RJ, Bean LR. Radiolucent halos associated with radiopaque composite resin restorations. *J Am Dent Assoc* 1989;118(5):595-7.
48. Tveit AB, Espelid I. Radiographic diagnosis of caries and marginal defects in connection with radiopaque composite fillings. *Dent Mater* 1986;2(4):159-62.
49. Berry HM, Jr. Cervical burnout and Mach band: two shadows of doubt in radiologic interpretation of carious lesions. *J Am Dent Assoc* 1983;106(5):622-5.
50. Welander U, McDavid WD, Higgins NM, Morris CR. The effect of viewing conditions on the perceptibility of radiographic details. *Oral Surg Oral Med Oral Pathol* 1983;56(6):651-4.
51. Preston-Martin S, White SC. Brain and salivary gland tumors related to prior dental radiography: implications for current practice. *J Am Dent Assoc* 1990;120(2):151-8.
52. Rohlin M, White SC. Comparative means of dose reduction in dental radiography. *Curr Opin Dent* 1992;2:1-9.
53. Wenzel A. Current trends in radiographic caries imaging. *Oral Surg Oral Med Oral Pathol Oral Radiol Endod* 1995;80(5):527-39.
54. Pitts NB, Kidd EA. The prescription and timing of bitewing radiography in the diagnosis and management of dental caries: contemporary recommendations. *Br Dent J* 1992;172(6):225-7.

55. Smith NJ. Selection criteria for dental radiography. *Br Dent J* 1992;173(4):120-1.
56. Schneiderman A, Elbaum M, Shultz T, et al. Assessment of dental caries with Digital Imaging Fiber-Optic Transillumination (DIFOTI): in vitro study. *Caries Res* 1997;31(2):103-10.
57. Pretty IA, Ellwood RP. The caries continuum: opportunities to detect, treat and monitor the re-mineralization of early caries lesions. *J Dent* 2013;41 Suppl 2:S12-21.
58. Sochtig F, Hickel R, Kuhnisch J. Caries detection and diagnostics with near-infrared light transillumination: clinical experiences. *Quintessence Int* 2014;45(6):531-8.
59. Kuhnisch J, Sochtig F, Pitchika V, et al. In vivo validation of near-infrared light transillumination for interproximal dentin caries detection. *Clin Oral Investig* 2015.
60. Pitts NB. Current methods and criteria for caries diagnosis in Europe. *J Dent Educ* 1993;57(6):409-14.
61. Bader JD, Brown JP. Dilemmas in caries diagnosis. *J Am Dent Assoc* 1993;124(6):48-50.
62. Pitts NB. The diagnosis of dental caries: 2. The detection of approximal, root surface and recurrent lesions. *Dent Update* 1991;18(10):436-8, 40-2.
63. Pitts NB, Longbottom C. Temporary tooth separation with special reference to the diagnosis and preventive management of equivocal approximal carious lesions. *Quintessence Int* 1987;18(8):563-73.
64. Mejare I, Grondahl HG, Carlstedt K, Grever AC, Ottosson E. Accuracy at radiography and probing for the diagnosis of proximal caries. *Scand J Dent Res* 1985;93(2):178-84.
65. Hintze H, Wenzel A, Danielsen B, Nyvad B. Reliability of visual examination, fibre-optic transillumination, and bite-wing radiography, and reproducibility of direct visual examination following tooth separation for the identification of cavitated carious lesions in contacting approximal surfaces. *Caries Res* 1998;32(3):204-9.

66. De Araujo FB, Rosito DB, Toigo E, dos Santos CK. Diagnosis of approximal caries: radiographic versus clinical examination using tooth separation. *Am J Dent* 1992;5(5):245-8.
67. Seddon RP. The detection of cavitation in carious approximal surfaces in vivo by tooth separation, impression and scanning electron microscopy. *J Dent* 1989;17(3):117-20.
68. Rimmer PA, Pitts NB. Temporary elective tooth separation as a diagnostic aid in general dental practice. *Br Dent J* 1990;169(3-4):87-92.
69. Martignon S, Ekstrand KR, Ellwood R. Efficacy of sealing proximal early active lesions: an 18-month clinical study evaluated by conventional and subtraction radiography. *Caries Res* 2006;40(5):382-8.
70. Alkilzy M, Berndt C, Meller C, Schidlowski M, Splieth C. Sealing of proximal surfaces with polyurethane tape: a two-year clinical and radiographic feasibility study. *J Adhes Dent* 2009;11(2):91-4.
71. Alkilzy M, Berndt C, Splieth CH. Sealing proximal surfaces with polyurethane tape: three-year evaluation. *Clin Oral Investig* 2011;15(6):879-84.
72. Martignon S, Tellez M, Santamaria RM, Gomez J, Ekstrand KR. Sealing distal proximal caries lesions in first primary molars: efficacy after 2.5 years. *Caries Res* 2010;44(6):562-70.
73. Martignon S, Ekstrand KR, Gomez J, Lara JS, Cortes A. Infiltrating/sealing proximal caries lesions: a 3-year randomized clinical trial. *J Dent Res* 2012;91(3):288-92.
74. Newbrun E. Problems in caries diagnosis. *Int Dent J* 1993;43(2):133-42.
75. Friedman J, Marcus MI. Transillumination of the oral cavity with use of fiber optics. *J Am Dent Assoc* 1970;80(4):801-9.
76. Vaarkamp J, ten Bosch JJ, Verdonschot EH, Bronkhorst EM. The real performance of bitewing radiography and fiber-optic transillumination in approximal caries diagnosis. *J Dent Res* 2000;79(10):1747-51.

77. Verdonschot EH, Bronkhorst EM, Wenzel A. Approximal caries diagnosis using fiber-optic transillumination: a mathematical adjustment to improve validity. *Community Dent Oral Epidemiol* 1991;19(6):329-32.
78. Holt RD, Azevedo MR. Fibre optic transillumination and radiographs in diagnosis of approximal caries in primary teeth. *Community Dent Health* 1989;6(3):239-47.
79. Mitropoulos CM. A comparison of fibre-optic transillumination with bitewing radiographs. *Br Dent J* 1985;159(1):21-3.
80. Wright GZ, Simon I. An evaluation of transillumination for caries detection in primary molars. *ASDC J Dent Child* 1972;39(3):199-202.
81. Peers A, Hill FJ, Mitropoulos CM, Holloway PJ. Validity and reproducibility of clinical examination, fibre-optic transillumination, and bite-wing radiology for the diagnosis of small approximal carious lesions: an in vitro study. *Caries Res* 1993;27(4):307-11.
82. Bin-Shuwaish M, Yaman P, Dennison J, Neiva G. The correlation of DIFOTI to clinical and radiographic images in Class II carious lesions. *J Am Dent Assoc* 2008;139(10):1374-81.
83. Ando M. Performance of Digital Imaging Fiber-optic Transillumination (DIFOTI) for Detection of Non-cavitated Primary Caries. Preliminary Report. 83rd General Session International Association for Dental Research Baltimore, Maryland: Moeller Printing Co., Inc; 2005. p. 12.
84. Young DA, Featherstone JD. Digital imaging fiber-optic trans-illumination, F-speed radiographic film and depth of approximal lesions. *J Am Dent Assoc* 2005;136(12):1682-7.
85. Lascala CA, Panella J, Marques MM. Analysis of the accuracy of linear measurements obtained by cone beam computed tomography (CBCT-NewTom). *Dentomaxillofac Radiol* 2004;33(5):291-4.
86. Ziegler CM, Woertche R, Brief J, Hassfeld S. Clinical indications for digital volume tomography in oral and maxillofacial surgery. *Dentomaxillofac Radiol* 2002;31(2):126-30.

87. Mozzo P, Procacci C, Tacconi A, Martini PT, Andreis IA. A new volumetric CT machine for dental imaging based on the cone-beam technique: preliminary results. *Eur Radiol* 1998;8(9):1558-64.
88. Danforth RA. Cone beam volume tomography: a new digital imaging option for dentistry. *J Calif Dent Assoc* 2003;31(11):814-5.
89. Sukovic P. Cone beam computed tomography in craniofacial imaging. *Orthod Craniofac Res* 2003;6 Suppl 1:31-6; discussion 179-82.
90. Scarfe WC. Imaging of maxillofacial trauma: evolutions and emerging revolutions. *Oral Surg Oral Med Oral Pathol Oral Radiol Endod* 2005;100(2 Suppl):S75-96.
91. Kalathingal SM, Mol A, Tyndall DA, Caplan DJ. In vitro assessment of cone beam local computed tomography for proximal caries detection. *Oral Surg Oral Med Oral Pathol Oral Radiol Endod* 2007;104(5):699-704.
92. Tsuchida R, Araki K, Okano T. Evaluation of a limited cone-beam volumetric imaging system: comparison with film radiography in detecting incipient proximal caries. *Oral Surg Oral Med Oral Pathol Oral Radiol Endod* 2007;104(3):412-6.
93. Haiter-Neto F, Wenzel A, Gotfredsen E. Diagnostic accuracy of cone beam computed tomography scans compared with intraoral image modalities for detection of caries lesions. *Dentomaxillofac Radiol* 2008;37(1):18-22.
94. Charuakkra A, Prapayasadok S, Janhom A, et al. Diagnostic performance of cone-beam computed tomography on detection of mechanically-created artificial secondary caries. *Imaging Sci Dent* 2011;41(4):143-50.
95. Kayipmaz S, Sezgin OS, Saricaoglu ST, Can G. An in vitro comparison of diagnostic abilities of conventional radiography, storage phosphor, and cone beam computed tomography to determine occlusal and approximal caries. *Eur J Radiol* 2011;80(2):478-82.
96. Senel B, Kamburoglu K, Ucok O, et al. Diagnostic accuracy of different imaging modalities in detection of proximal caries. *Dentomaxillofac Radiol* 2010;39(8):501-11.

97. Qu X, Li G, Zhang Z, Ma X. Detection accuracy of in vitro approximal caries by cone beam computed tomography images. *Eur J Radiol* 2011;79(2):e24-7.
98. Young SM, Lee JT, Hodges RJ, et al. A comparative study of high-resolution cone beam computed tomography and charge-coupled device sensors for detecting caries. *Dentomaxillofac Radiol* 2009;38(7):445-51.
99. Cheng JG, Zhang ZL, Wang XY, et al. Detection accuracy of proximal caries by phosphor plate and cone-beam computerized tomography images scanned with different resolutions. *Clin Oral Investig* 2012;16(4):1015-21.
100. Rathore S, Tyndall D, Wright J, Everett E. Ex vivo comparison of Galileos cone beam CT and intraoral radiographs in detecting occlusal caries. *Dentomaxillofac Radiol* 2012;41(6):489-93.
101. Wenzel A, Hirsch E, Christensen J, et al. Detection of cavitated approximal surfaces using cone beam CT and intraoral receptors. *Dentomaxillofac Radiol* 2013;42(1):39458105.
102. Valizadeh S, Tavakkoli MA, Karimi Vasigh H, Azizi Z, Zarrabian T. Evaluation of Cone Beam Computed Tomography (CBCT) System: Comparison with Intraoral Periapical Radiography in Proximal Caries Detection. *J Dent Res Dent Clin Dent Prospects* 2012;6(1):1-5.
103. Krzyzostaniak J, Surdacka A, Kulczyk T, Dyszkiewicz-Konwinska M, Owecka M. Diagnostic accuracy of cone beam computed tomography compared with intraoral radiography for the detection of noncavitated occlusal carious lesions. *Caries Res* 2014;48(5):461-6.
104. Tarim Ertas E, Kucukyilmaz E, Ertas H, Savas S, Yircali Atici M. A Comparative Study of Different Radiographic Methods for Detecting Occlusal Caries Lesions. *Caries Res* 2014;48(6):566-74.
105. Zhang ZL, Qu XM, Li G, Zhang ZY, Ma XC. The detection accuracies for proximal caries by cone-beam computerized tomography, film, and phosphor plates. *Oral Surg Oral Med Oral Pathol Oral Radiol Endod* 2011;111(1):103-8.
106. Sansare K, Singh D, Sontakke S, et al. Should cavitation in proximal surfaces be reported in cone beam computed tomography examination? *Caries Res* 2014;48(3):208-13.

107. Wenzel A. Radiographic display of carious lesions and cavitation in approximal surfaces: Advantages and drawbacks of conventional and advanced modalities. *Acta Odontol Scand* 2014;72(4):251-64.
108. Huang D, Swanson EA, Lin CP, et al. Optical coherence tomography. *Science* 1991;254(5035):1178-81.
109. Shimada Y, Sadr A, Sumi Y, Tagami J. Application of Optical Coherence Tomography (OCT) for Diagnosis of Caries, Cracks, and Defects of Restorations. *Curr Oral Health Rep* 2015;2(2):73-80.
110. Pierce MC, Strasswimmer J, Hyle Park B, Cense B, De Boer JF. Birefringence measurements in human skin using polarization-sensitive optical coherence tomography. *J Biomed Opt* 2004;9(2):287-91.
111. Mamalis A, Ho D, Jagdeo J. Optical Coherence Tomography Imaging of Normal, Chronologically Aged, Photoaged and Photodamaged Skin: A Systematic Review. *Dermatol Surg* 2015;41(9):993-1005.
112. Uno K, Koike T, Shimosegawa T. Recent development of optical coherence tomography for preoperative diagnosis of esophageal malignancies. *World J Gastrointest Endosc* 2015;7(9):872-80.
113. Pinilla I, Fernandez-Sanchez L, Segura FJ, et al. Long time remodeling during retinal degeneration evaluated by optical coherence tomography, immunocytochemistry and fundus autofluorescence. *Exp Eye Res* 2015.
114. Shimada Y, Nakagawa H, Sadr A, et al. Noninvasive cross-sectional imaging of proximal caries using swept-source optical coherence tomography (SS-OCT) in vivo. *J Biophotonics* 2014;7(7):506-13.
115. Hariri I, Sadr A, Shimada Y, Tagami J, Sumi Y. Effects of structural orientation of enamel and dentine on light attenuation and local refractive index: an optical coherence tomography study. *J Dent* 2012;40(5):387-96.
116. Imai K, Shimada Y, Sadr A, Sumi Y, Tagami J. Noninvasive cross-sectional visualization of enamel cracks by optical coherence tomography in vitro. *J Endod* 2012;38(9):1269-74.



117. Makishi P, Shimada Y, Sadr A, Tagami J, Sumi Y. Non-destructive 3D imaging of composite restorations using optical coherence tomography: marginal adaptation of self-etch adhesives. *J Dent* 2011;39(4):316-25.
118. Bakhsh TA, Sadr A, Shimada Y, Tagami J, Sumi Y. Non-invasive quantification of resin-dentin interfacial gaps using optical coherence tomography: validation against confocal microscopy. *Dent Mater* 2011;27(9):915-25.
119. Hibst R, Paulus R, Lussi A. Detection of Occlusal Caries by Laser Fluorescence: Basic and Clinical Investigations. *Medical Laser Application* 2001;16(3):9.
120. Konig K, Flemming G, Hibst R. Laser-induced autofluorescence spectroscopy of dental caries. *Cell Mol Biol (Noisy-le-grand)* 1998;44(8):1293-300.
121. Lussi A, B A-M. Additional diagnostic measures. In: O F, E K, editors. *Dental Caries The Disease and its Clinical Management*. 2 ed. Oxford: Blackwell Munksgaard 2008. p. 93-94.
122. Lussi A, Hibst R, Paulus R. DIAGNOdent: an optical method for caries detection. *J Dent Res* 2004;83 Spec No C:C80-3.
123. Ribeiro AA, Purger F, Rodrigues JA, et al. Influence of contact points on the performance of caries detection methods in approximal surfaces of primary molars: an in vivo study. *Caries Res* 2015;49(2):99-108.
124. Bader JD, Shugars DA. A systematic review of the performance of a laser fluorescence device for detecting caries. *J Am Dent Assoc* 2004;135(10):1413-26.
125. Baum G, Greenwood I, Slawski S, Smirnow R. Observation of internal structures of teeth by ultrasonography. *Science* 1963;139(3554):495-6.
126. Laird WR, Walmsley AD. Ultrasound in dentistry. Part 1--Biophysical interactions. *J Dent* 1991;19(1):14-7.
127. Marotti J, Heger S, Tinschert J, et al. Recent advances of ultrasound imaging in dentistry--a review of the literature. *Oral Surg Oral Med Oral Pathol Oral Radiol* 2013;115(6):819-32.

128. Matalon S, Feuerstein O, Kaffe I. Diagnosis of approximal caries: bite-wing radiology versus the Ultrasound Caries Detector. An in vitro study. *Oral Surg Oral Med Oral Pathol Oral Radiol Endod* 2003;95(5):626-31.
129. Matalon S, Feuerstein O, Calderon S, Mittleman A, Kaffe I. Detection of cavitated carious lesions in approximal tooth surfaces by ultrasonic caries detector. *Oral Surg Oral Med Oral Pathol Oral Radiol Endod* 2007;103(1):109-13.
130. Neuhaus KW, Ciucchi P, Rodrigues JA, et al. Diagnostic performance of a new red light LED device for approximal caries detection. *Lasers Med Sci* 2014.
131. Neuhaus KW, Ciucchi P, Rodrigues JA, et al. Diagnostic performance of a new red light LED device for approximal caries detection. *Lasers Med Sci* 2015;30(5):1443-7.
132. Nicolaides L, Feng C, Mandelis A, Abrams SH. Quantitative dental measurements by use of simultaneous frequency-domain laser infrared photothermal radiometry and luminescence. *Appl Opt* 2002;41(4):768-77.
133. Landsberg PT. *Thermodynamics and statistical mechanics*. Dover ed. New York: Dover Publications; 1990.
134. Nicolaides L, Mandelis A, Abrams SH. Novel dental dynamic depth profilometric imaging using simultaneous frequency-domain infrared photothermal radiometry and laser luminescence. *J Biomed Opt* 2000;5(1):31-9.
135. Jeon RJ, Han C, Mandelis A, Sanchez V, Abrams SH. Diagnosis of pit and fissure caries using frequency-domain infrared photothermal radiometry and modulated laser luminescence. *Caries Res* 2004;38(6):497-513.
136. Jeon RJ, Matvienko A, Mandelis A, et al. Detection of interproximal demineralized lesions on human teeth in vitro using frequency-domain infrared photothermal radiometry and modulated luminescence. *J Biomed Opt* 2007;12(3):034028.
137. Jan J, Wan Bakar WZ, Mathews SM, et al. Proximal caries lesion detection using the Canary Caries Detection System: an in vitro study. *J Investig Clin Dent* 2015.

138. Baelum V, Nyvad B, Gröndahl H-G, Fejerskov O. The foundations of good diagnostic practice. In: Fejerskov O, Kidd EAM, editors. *Dental Caries the Disease and its Clinical Management*. 2nd ed. Oxford: Blackwell Munksgaard; 2008. p. 103-20.
139. Ricketts DN, Watson TF, Liepins PJ, Kidd EA. A comparison of two histological validating techniques for occlusal caries. *J Dent* 1998;26(2):89-96.
140. Jablonski-Momeni A, Stachniss V, Ricketts DN, Heinzl-Gutenbrunner M, Pieper K. Reproducibility and accuracy of the ICDAS-II for detection of occlusal caries in vitro. *Caries Res* 2008;42(2):79-87.
141. Mitropoulos P, Rahiotis C, Stamatakis H, Kakaboura A. Diagnostic performance of the visual caries classification system ICDAS II versus radiography and micro-computed tomography for proximal caries detection: an in vitro study. *J Dent* 2010;38(11):859-67.
142. Davis GR, Wong FS. X-ray microtomography of bones and teeth. *Physiol Meas* 1996;17(3):121-46.
143. Hahn SK, Kim JW, Lee SH, et al. Microcomputed tomographic assessment of chemomechanical caries removal. *Caries Res* 2004;38(1):75-8.
144. Huang TT, Jones AS, He LH, Darendeliler MA, Swain MV. Characterisation of enamel white spot lesions using X-ray micro-tomography. *J Dent* 2007;35(9):737-43.
145. Kim I, Paik KS, Lee SP. Quantitative evaluation of the accuracy of micro-computed tomography in tooth measurement. *Clin Anat* 2007;20(1):27-34.
146. Postnov AA, Vinogradov AV, Van Dyck D, Saveliev SV, De Clerck NM. Quantitative analysis of bone mineral content by x-ray microtomography. *Physiol Meas* 2003;24(1):165-78.
147. Stauber M, Muller R. Micro-computed tomography: a method for the non-destructive evaluation of the three-dimensional structure of biological specimens. *Methods Mol Biol* 2008;455:273-92.
148. Willmott NS, Wong FS, Davis GR. An X-ray microtomography study on the mineral concentration of carious dentine removed during cavity preparation in deciduous molars. *Caries Res* 2007;41(2):129-34.

149. Wong FS, Anderson P, Fan H, Davis GR. X-ray microtomographic study of mineral concentration distribution in deciduous enamel. *Arch Oral Biol* 2004;49(11):937-44.
150. Anderson P, Elliott JC, Bose U, Jones SJ. A comparison of the mineral content of enamel and dentine in human premolars and enamel pearls measured by X-ray microtomography. *Arch Oral Biol* 1996;41(3):281-90.
151. Salome M, Peyrin F, Cloetens P, et al. A synchrotron radiation microtomography system for the analysis of trabecular bone samples. *Med Phys* 1999;26(10):2194-204.
152. Koob A, Sanden E, Hassfeld S, Staehle HJ, Eickholz P. Effect of digital filtering on the measurement of the depth of proximal caries under different exposure conditions. *Am J Dent* 2004;17(6):388-93.
153. Soviero VM, Leal SC, Silva RC, Azevedo RB. Validity of MicroCT for in vitro detection of proximal carious lesions in primary molars. *J Dent* 2012;40(1):35-40.
154. Ludwig-Maximilian Diagnosis of interproximal caries in a permanent premolar. 2016. "<http://www.diagnocam.com/EN/Productinfo/Examples.aspx>".
155. Abdelaziz M, Krejci I. DIAGNOcam--a Near Infrared Digital Imaging Transillumination (NIDIT) technology. *Int J Esthet Dent* 2015;10(1):158-65.
156. Wenzel A, Borg E, Hintze H, Grondahl HG. Accuracy of caries diagnosis in digital images from charge-coupled device and storage phosphor systems: an in vitro study. *Dentomaxillofac Radiol* 1995;24(4):250-4.
157. Ando M. Performance of Digital Imaging Fiber-optic Transillumination (DIFOTI) for Detection of Non-cavitated Primary Caries. Preliminary Report. In: Stookey G, editor. 83rd International Association for Dental Research Baltimore, Maryland: TheraMetric Technologies Inc.; 2005. p. 41-52.
158. Landis JR, Koch GG. The measurement of observer agreement for categorical data. *Biometrics* 1977;33(1):159-74.
159. Nyvad B, Machiulskiene V, Baelum V. Construct and predictive validity of clinical caries diagnostic criteria assessing lesion activity. *J Dent Res* 2003;82(2):117-22.

160. Zandona AF, Zero DT. Diagnostic tools for early caries detection. *J Am Dent Assoc* 2006;137(12):1675-84; quiz 730.
161. Rainer Haak, Wicht MJ. Radiographic and Other Additional Diagnostic Methods. In: Hendrik Meyer-Lueckel, Sebastian Paris, Ekstrand KR, editors. *Caries Management-Science and Clinical Practice*. Germany: Thieme Medical Publisher, Inc; 2013. p. 86-101.
162. Jones RS, D Fried. Attenuation of 1310- and 1550-nm laser lightthrough sound dental enamel. Paper presented at: SPIE the International Society for Optical Engineering ; v. 4610, 2002; San Jose. CA, USA.
163. Fried D, Glena RE, Featherstone JD, Seka W. Nature of light scattering in dental enamel and dentin at visible and near-infrared wavelengths. *Appl Opt* 1995;34(7):1278-85.
164. Daniel Fried, Michal Staninec, Darling CL. Near-Infrared Imaging of Dental Decay at 1310 nm. *J Laser Dent* 2010;18(1):8-16.
165. Staninec M, Lee C, Darling CL, Fried D. In vivo near-IR imaging of approximal dental decay at 1,310 nm. *Lasers Surg Med* 2010;42(4):292-8.
166. Astvaldsdottir A, Ahlund K, Holbrook WP, de Verdier B, Tranaeus S. Approximal Caries Detection by DIFOTI: In Vitro Comparison of Diagnostic Accuracy/Efficacy with Film and Digital Radiography. *Int J Dent* 2012;2012:326401.
167. Darling CL, Fried D. Real-time near IR (1310 nm) imaging of CO2 laser ablation of enamel. *Opt Express* 2008;16(4):2685-93.
168. Bosch JJt. Light Scattering and Related Methods in Caries Diagnosis. Paper presented at: The First Annual Indiana Conference. Indiana University School of Dentistry, 1996; Indiana University School of Dentistry.
169. Wenzel A. Dental caries. In: White S, Pharoah M, editors. *Oral radiology. Principles and interpretation*. 5th ed. St. Louis: Mosby; 2004. p. 297-313.
170. Pitts NB, Kidd EA. 'Selection criteria for dental radiography'. *Br Dent J* 1992;173(7):227.

171. Woelfel JB, Scheid RC. *Dental Anatomy. Its Relevance to Dentistry*. 6th ed. Baltimore: Lippincott Williams & Wilkins; 2001.
172. Novaes TF, Matos R, Raggio DP, et al. Influence of the discomfort reported by children on the performance of approximal caries detection methods. *Caries Res* 2010;44(5):465-71.
173. Novaes TF, Matos R, Braga MM, et al. Performance of a pen-type laser fluorescence device and conventional methods in detecting approximal caries lesions in primary teeth--in vivo study. *Caries Res* 2009;43(1):36-42.
174. Shoaib L, Deery C, Ricketts DN, Nugent ZJ. Validity and reproducibility of ICDAS II in primary teeth. *Caries Res* 2009;43(6):442-8.
175. Brantley CF, Bader JD, Shugars DA, Nesbit SP. Does the cycle of reresoration lead to larger restorations? *J Am Dent Assoc* 1995;126(10):1407-13.
176. Elderton RJ. Preventive (evidence-based) approach to quality general dental care. *Med Princ Pract* 2003;12 Suppl 1:12-21.

APPENDIX

Performance of Near Infrared Digital Imaging Transillumination for Detection of Non-cavitated Approximal Caries

Timeline & Examination Manual



## Participants

1- Masatoshi Ando (PI)	Examiner 1
2- Anderson T Hara	Examiner 2
3- Ana Gossweiler	Examiner 3
4- George J. Eckert	Biostatistician
5- Naif Abogazalah	Facilitator

### Objectives of the Study

- 1) To evaluate the ability of the Near Infrared Digital Imaging Transillumination (NIDIT) system to detect non-cavitated enamel and dentin approximal caries lesions.
- 2) To determine the correlation among NIDIT, visual examination: International Caries Detection and Assessment System (ICDAS), Digital Radiography (DR), and Digital Imaging Fiber-Optic Trans-Illumination (DIFOTI).

A Flow Chart of the Study

Teeth Selection

Initial Microfocus Computed Tomography ( $\mu$ -CT) Image  
Acquisition for lesion depth evaluation

Model Assembling

Main  $\mu$ -CT Image Acquisition to establish gold standard

Training

Calibration

Repeated Calibration

Statistical Analysis after Calibration

Main Examination

Repeated Examination

Statistical Analysis

## Project Schedule for Training, Calibration, Main Examination and Repeated Examination

Sessions from Nov 1, 2015 to Dec 18, 2015

All examinations and hands on training will take place at the Early Caries Detection

Laboratory

Room #131, Indiana University Oral Health Research Building.

	Date	Time	Participant	Method	Note
Training	Day 1 .....	8:00 - 8:50 AM	All Examiners	ICDSD NIDIT DR DIFOTI	Theoretical explanation and discussion using PowerPoint presentation including photograph examples. It will cover the criteria of ICDAS, DR, NIDIT and DIFOTI.
		9:00 - 12:00 AM	All Examiners	ICDSD NIDIT DR DIFOTI	Hands on training session and discussion covering all detection methods. N = 8 (sound=2), (E1=2), (E2=2) & (D1 = 2).
Calibration	Day 2 .....	1:00 - 2:00 PM	Examiner (...)	ICDAS	Examination of 12 approximal sites of assembled teeth.
		2:00 - 3:00 PM	Examiner (...)		
		3:00 - 4:00 PM	Examiner (...)		
	.....	8:00 - 9:00 AM	Examiner (...)	NIDIT	Examination of 12 approximal sites of assembled teeth.
		9:00 - 10:00 AM	Examiner (...)		
		10:00-11:00 AM	Examiner (...)		
.....	.....	1:00 - 2:00 PM	Examiner (...)	DR	Examination of 12 approximal sites of assembled teeth.
		2:00 - 3:00 PM	Examiner (...)		
		3:00 - 4:00 PM	Examiner (...)		

Project Schedule Continue						
Calibration	Day 3	8:00 - 9:00 AM	Examiner (...)	DIFOTI	Examination of 12 approximal sites of assembled teeth.	
		9:00 -10:00 AM	Examiner (...)			
		10:00-11:00 AM	Examiner (...)			
Repeated Calibration	.....	1:00 - 2:00 PM	Examiner (...)	ICDAS	Repeated examination of 12 approximal sites of assembled teeth.	
		2:00 - 3:00 PM	Examiner (...)			
		3:00 - 4:00 PM	Examiner (...)			
	Day 4	.....	8:00 - 9:00 AM	Examiner (...)	NIDIT	Repeated examination of 12 approximal sites of assembled teeth.
			9:00 -10:00 AM	Examiner (...)		
			10:00-11:00 AM	Examiner (...)		
	.....	.....	1:00 - 2:00 PM	Examiner (...)	DR	Repeated examination of 12 approximal sites of assembled teeth.
			2:00 - 3:00 PM	Examiner (...)		
			3:00 - 4:00 PM	Examiner (...)		
	Day 5	....	8:00 - 9:00 AM	Examiner (...)	DIFOTI	Repeated examination of 12 approximal sites of assembled teeth.
			9:00 -10:00 AM	Examiner (...)		
			10:00-11:00 AM	Examiner (...)		
Statistical Analysis: One Week						

Project Schedule Continue					
Main Examination	Day 6 .....	8:00 - 10:00 AM	Examiner (...)	ICDAS	Examination of 30 approximal sites of assembled teeth.
		10:00 AM-12:00 PM	Examiner (...)		
		1:00 - 3:00 PM	Examiner (...)		
	Day 7	8:00 - 10:00 AM	Examiner (...)	NIDIT	Examination of 30 approximal sites of assembled teeth.
		10:00 AM-12:00 PM	Examiner (...)		
		1:00 - 3:00 PM	Examiner (...)		
	Day 8 ....	8:00 - 10:00 AM	Examiner (...)	DR & DIFOTI	Examination of 30 approximal sites of assembled teeth.
		10:00 AM-12:00 PM	Examiner (...)		
		1:00 - 3:00 PM	Examiner (...)		
Tow Weeks					
Repeated Examination	Day 9 .....	8:00 - 10:00 AM	Examiner (...)	ICDAS	Repeated examination of 30 approximal sites of assembled teeth.
		10:00 AM-12:00 PM	Examiner (...)		
		1:00 - 3:00 PM	Examiner (...)		
	Day 10	8:00 - 10:00 AM	Examiner (...)	NIDIT	Repeated examination of 30 approximal sites of assembled teeth.
		10:00 AM-12:00 PM	Examiner (...)		
		1:00 - 3:00 PM	Examiner (...)		
	Day 11	8:00 - 10:00 AM	Examiner (...)	DR & DIFOTI	Repeated examination of 30 approximal sites of assembled teeth.
		10:00 AM-12:00 PM	Examiner (...)		
		1:00 - 3:00 PM	Examiner (...)		
Statistical Analysis					

#### Instructions for ICDAS Examination Procedure:

Sound, as well as carious, premolars with approximal non-cavitated caries lesions were assembled for the examination. The test teeth were kept in a container with saturated gauze with 0.1% thymol solution to maintain humidity. The teeth are mounted on Lego<sup>®</sup> blocks using fibered pink resin. The station is equipped with a light unit and air syringe. On the bench, you will find a front surface mirror, explorer, and an assembled extracted premolar, which will remain fixed during the whole time, and it will serve as an adjacent to the test tooth. The facilitator will take the responsibility to replace and mount each test-tooth during the examination. The examiner will examine the approximal site of the test tooth in contact with the adjacent tooth and he will report the score verbally to the facilitator.

### ICDAS Scoring Criteria for Approximal Caries

0 = Sound tooth surface. Show no evidence of visible caries when viewed clean and after prolonged air-drying (5 seconds). Surfaces with developmental defects such as enamel hypomineralization (including fluorosis); tooth wear (attrition, abrasion and erosion), and extrinsic or intrinsic stains will be recorded as sound.

1 = First visual changes in Enamel. Opacity or discoloration not visible on wet surface, but distinctly visible after 5 seconds of air-drying. Usually seen from lingual/ buccal or from occlusal.

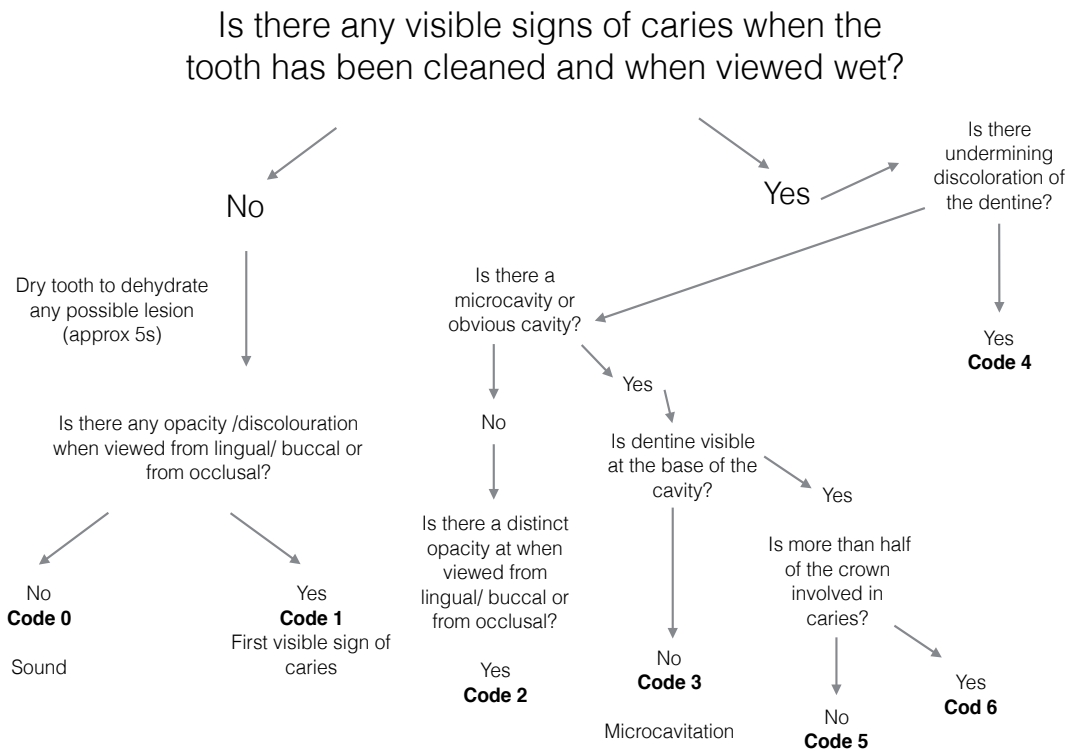
2 = Distinct visual change in enamel. Opacity or discoloration distinctly visible on wet surface. Usually seen from lingual/ buccal or from occlusal as a shadow confined to enamel.

3 = Localized enamel breakdown with no visible dentin. Caries loss of enamel integrity viewed from buccal and lingual direction. Confirmation can be assisted with use of the explorer gently across the surface to confirm enamel micro-cavity/discontinuity.

4 = Non-cavitated surface with underlying dentin dark shadowing. It appears as appears as a shadow of grey, blue or brown discolored dentin. Directly seen from lingual /buccal and when a discolored dentin is visible through the occlusal marginal ridge.



Decision Tree for ICDAS Scoring

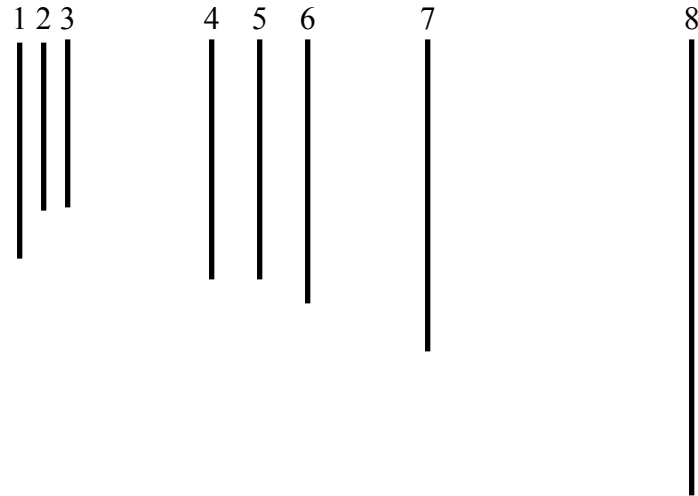


## ICDAS Scoring Criteria summary

- 0 = Sound tooth surface
- 1 = White spot lesion under wet condition
- 2 = White spot lesion under a dry condition
- 3 = Localized enamel breakdown
- 4 = Lesion with dentin shadowing

## Near Infrared Digital Imaging Transillumination (NIDIT)

## System Components



1	Aperture for laser beam	2	Opening for camera window
3	Occlusal Tip	4	Ring Switch
5	Control Button 1	6	Control Button 2
6	Headpiece	8	USB cable to connect to computer

## Instructions for NIDIT Examination Procedure

The facilitator will take the responsibility to replace and mount each test tooth during the examination. The steps to take NIDIT images are as follow:

- 1- Place the light aperture and make it contact the gingiva and monitor the live picture.
- 2- If the picture is too bright, bring the tip little down apically. If it is too dark you may bring the tip up occlusal
- 3- Tip the probe slightly if needed.
- 4- When you are satisfied with the captured image, press the ring switch (4) to freeze the image or press for three seconds to save the image.
- 5- Pleas, report the score to the facilitator.

## The scoring criteria for NIDIT system

0	No Shadowing.
E <sub>1</sub>	Shadow in outer half of enamel.
E <sub>2</sub>	Shadow in inner half of enamel, but not to DEJ.
D <sub>1</sub>	Shadow extended to DEJ, but not beyond outer one third of dentin.

### Instructions for Digital Radiography Examination Procedure

Mounted teeth were radiographed. The images will be viewed in a dark room on a digital screen. The facilitator will be responsible for viewing the images and writing the scores.

Please, report the approximal surface score of the defined teeth to the facilitator.

### Radiographic Scoring Criteria

0	No Radiolucency.
E <sub>1</sub>	Radiolucency in the outer half of the enamel.
E <sub>2</sub>	Radiolucency in the inner half of the enamel and not beyond the DEJ.
D <sub>1</sub>	Radiolucency in the outer one-third of dentin.

## Instructions for Digital Imaging Fiber-Optic Trans-Illumination (DIFOTI) Examination

### Procedure

DIFOTI images were previously obtained. For each tooth, three images are available to obtain a view for the occlusal, buccal and lingual surfaces. The facilitator will be responsible for viewing the images and writing the score. Please, report the approximal surface score of the defined teeth to the facilitator.

### DIFOTI Scoring Criteria

Score	Criterion
0	No caries
1	Probably no caries present
2	Not sure
3	Probably caries is present
4	Caries present

### DIFOTI Image Views of teeth with approximal caries lesion

Occlusal	Buccal	Lingual

ABSTRACT

PERFORMANCE OF NEAR INFRARED DIGITAL IMAGING  
TRANSILLUMINATION FOR DETECTION OF  
NON-CAVITATED APPROXIMAL CARIES

by

Naif Nabel F Abogazalah

Indiana University School of Dentistry  
Indianapolis, Indiana

Objective: The objectives of this *in-vitro* study were: 1) to evaluate the ability of Near-Infrared Digital Imaging Transillumination (NIDIT) to detect non-cavitated approximal caries lesions; and 2) to compare the performance among NIDIT, Digital Radiography (DR), Digital Imaging Fiber-Optic Trans-Illumination (DIFOTI) and International Caries Detection and Assessment System (ICDAS).



Methods: Thirty human extracted premolars were selected. The approximal surface status ranged from sound to surfaces with non-cavitated caries lesions into the outer one-third of the dentin. Lesion depth was determined by micro-computed tomography ( $\mu$ -CT) and used as a gold standard. Teeth were mounted in a custom-made device to simulate approximal contact. ICDAS, DR, DIFOTI and NIDIT examinations were performed and repeated by three trained and calibrated examiners. Sensitivity, specificity, area under ROC curve (Az), inter- and intra-class correlation coefficients (ICCs) of each method, and correlation among the methods were determined.

Results: ICCs for intra-/inter-examiner agreement were almost perfect for DIFOTI (0.85/0.83), substantial for ICDAS (0.79/0.72) and NIDIT (0.69/0.64), and moderate for DR (0.52/0.48). Sensitivity/specificity for DIFOTI, ICDAS, DR, and NIDIT were 0.91/0.69, 0.89/0.83, 0.50/0.64, and 0.68/0.93, respectively. Az of DR (0.61) was significantly lower than that of DIFOTI (0.91,  $p = 0.002$ ) and ICDAS (0.90,  $p = 0.005$ ), but was not significantly different from NIDIT (0.81,  $p = 0.052$ ). DIFOTI, ICDAS, and NIDIT were not significantly different from each other ( $p > 0.13$ ). Spearman correlation coefficients for DIFOTI (0.79,  $p < 0.001$ ), ICDAS (0.74,  $p < 0.001$ ), and NIDIT (0.65,  $p < 0.001$ ) demonstrated a moderate association with  $\mu$ -CT, while that of DR suggested no association (0.19,  $p = 0.289$ ).

Conclusion: Within the limitations of this *in-vitro* study, NIDIT system demonstrated a potential for early approximal caries detection. ICDAS, DIFOTI, and NIDIT were superior to DR in terms of validity and reliability.

## CORRICULUM VITAE

September 29, 1986	Born in Abha, Kingdom of Saudi Arabia
July 2011	BDS, King Khalid University, College of Dentistry, Abha, Kingdom of Saudi Arabia
Aug 2011	Teaching Assistant, King Khalid University, College of Dentistry, Kingdom of Saudi Arabia
July 2016	MSD, Operative Dentistry Preventive Dentistry, Indiana University School of Dentistry, Indianapolis, Indiana,

#### Professional Organizations

The International Association of Dental Research  
American Association of Dental Research  
American Academy of Operative Dentistry  
Saudi Dental Society